Supplementary information for

# Global Methane Budget: 2000-2020


Marielle Saunois[1] Adrien Martinez[1] Benjamin Poulter[2] Zhen Zhang[3,4]
Peter A. Raymond[5] Pierre Regnier[6] Josep G. Canadell[7] Robert B. Jackson[8]
Prabir K. Patra[9,10] Philippe Bousquet[1] Philippe Ciais[1] Edward J. Dlugokencky[11]
Xin Lan[11,12] George H. Allen[13] David Bastviken[14] David J. Beerling[15]
Dmitry A. Belikov[16] Donald R. Blake[17] Simona Castaldi[18] Monica Crippa[19,20]
Bridget R. Deemer[21] Fraser Dennison[22] Giuseppe Etiope[23,24] Nicola Gedney[25]
Lena Höglund-Isaksson[26] Meredith A. Holgerson[27] Peter O. Hopcroft[28]
Gustaf Hugelius[29] Akihiko Ito[30] Atul K. Jain3 [31] Rajesh Janardanan[32]
Matthew S. Johnson[33] Thomas Kleinen[34] Paul B. Krummel[22] Ronny Lauerwald[35]
Tingting Li[36] Xiangyu Liu[37] Kyle C. McDonald[38] Joe R. Melton[39] Jens Mühle[40]
Jurek Müller[41] Fabiola Murguia-Flores[42] Yosuke Niwa[32,43] Sergio Noce[44]
Shufen Pan[45] Robert J. Parker[46] Changhui Peng[47,48] Michel Ramonet[1]
William J. Riley[49] Gerard Rocher-Ros[50] Judith A. Rosentreter[51] Motoki Sasakawa[32]
Arjo Segers[52] Steven J. Smith[53,54] Emily H. Stanley[55] Joël Thanwerdas[56,*]
Hanqin Tian[57] Aki Tsuruta[58] Francesco N. Tubiello[59] Thomas S. Weber[60]
Guido R. van der Werf[61] Douglas E. J. Worthy[62] Yi Xi[1] Yukio Yoshida[32]
Wenxin Zhang[63] Bo Zheng[64,65] Qing Zhu[49] Qiuan Zhu[66] and Qianlai Zhuang[3]

[1]Laboratoire des Sciences du Climat et de l'Environnement, LSCE-IPSL (CEA-CNRS-UVSQ), Université Paris-Saclay 91191 Gif-sur-Yvette, France
[2]NASA Goddard Space Flight Center, Biospheric Science Laboratory, Greenbelt, MD 20771, USA
[3]National Tibetan Plateau Data Center (TPDC), State Key Laboratory of Tibetan Plateau Earth System, Environment and Resource (TPESER), Institute of Tibetan Plateau Research, Chinese Academy of Sciences, Beijing, 100101, China
[4]Earth System Science Interdisciplinary Center, University of Maryland, College Park, MD 20740, USA
[5]Yale School of the Environment, Yale University, New Haven, CT 06511, USA.
[6]Department Geoscience, Environment Society (BGEOSYS), Université Libre de Bruxelles, 1050 Bruxelles, Belgium
[7]Global Carbon Project, CSIRO Environment, Canberra, ACT 2601, Australia
[8]Department of Earth System Science, Woods Institute for the Environment, and Precourt Institute for Energy, Stanford University, Stanford, CA 94305-2210, USA
[9]Research Institute for Global Change, JAMSTEC, 3173-25 Showa-machi, Kanazawa, Yokohama, 236-0001, Japan
[10]Research Institute for Humanity and Nature, Kyoto 6038047, Japan
[11]NOAA Global Monitoring Laboratory, 325 Broadway, Boulder, CO 80305, USA
[12]Cooperative Institute for Research in Environmental Sciences, University of Colorado Boulder, CO 80303, USA
[13]Department of Geosciences, Virginia Polytechnic Institute and State University, Blacksburg, VA, USA
[14]Department of Thematic Studies – Environmental Change, Linköping University, 581 83 Linköping, Sweden
[15]School of Biosciences, University of Sheffield, U.K.
[16]Center for Environmental Remote Sensing, Chiba University, Chiba, 263-8522, Japan
[17]Department of Chemistry, University of California Irvine, 570 Rowland Hall, Irivine, CA 92697, USA

[18]Dipartimento di Scienze Ambientali, Biologiche e Farmaceutiche, Università degli Studi della Campania Luigi Vanvitelli, via Vivaldi 43, 81100 Caserta, Italy
[19]European Commission, Joint Research Centre (JRC), Ispra, Italy
[20]Unisystems S.A., Milan, Italy
[21]U.S. Geological Survey, Southwest Biological Science Center, Flagstaff, AZ, USA
[22]CSIRO Environment, Aspendale, Victoria 3195, Australia
[23]Istituto Nazionale di Geofisica e Vulcanologia, Sezione Roma 2, via V. Murata 605 00143 Rome, Italy
[24]Faculty of Environmental Science and Engineering, Babes Bolyai University, Cluj-Napoca, Romania
[25] Met Office Hadley Centre, Joint Centre for Hydrometeorological Research, Maclean Building, Wallingford OX10 8BB, UK
[26]Pollution Management Group (PM), International Institute for Applied Systems Analysis (IIASA), 2361 Laxenburg, Austria
[27] Department of Ecology  Evolutionary Biology, Cornell University, Ithaca, NY, USA
[28] School of Geography, Earth  Environmental Sciences, University of Birmingham, U.K.
[29] Department of Physical Geography and Bolin Centre for Climate Research, Stockholm University, 106 91 Stockholm, Sweden
[30] Graduate School of Agricultural and Life Sciences, The University of Tokyo, Tokyo, Japan
[31] Department of Atmospheric Sciences, University of Illinois, Urbana, IL 61821, USA
[32] Earth System Division, National Institute for Environmental Studies (NIES), Onogawa 16-2, Tsukuba, Ibaraki 305-8506, Japan
[33]Earth Science Division, NASA Ames Research Center, Moffett Field, CA USA.
[34]Max Planck Institute for Meteorology, Bundesstraße 53, 20146 Hamburg, Germany
[35] Université Paris-Saclay, INRAE, AgroParisTech, UMR EcoSys, Palaiseau, France
[36]LAPC, Institute of Atmospheric Physics, Chinese Academy of Sciences, Beijing, 100029, China
[37]Department of Earth, Atmospheric, and Planetary Sciences, Purdue University, West Lafayette, IN, USA
[38]Department of Earth and Atmospheric Sciences, City College of New York, City University of New York, NY, USA
[39]Climate Research Division, Environment and Climate Change Canada, Victoria, BC, V8W 2Y2, Canada
[40]Scripps Institution of Oceanography, University of California San Diego, La Jolla, CA, 92037, USA
[41]Climate and Environmental Physics, Physics Institute and Oeschger Centre for Climate Change Research, University of Bern, Sidlerstr. 5, 3012 Bern, Switzerland
[42]Instituto de Investigaciones en Ecología y Sustentabilidad, Universidad Nacional Autónoma de México, Morelia, Mexico
[43]Department of Climate and Geochemistry Research, Meteorological Research Institute (MRI), Nagamine 1-1, Tsukuba, Ibaraki 305-0052, Japan
[44]CMCC Foundation - Euro-Mediterranean Center on Climate Change, Italy.
[45]Department of Engineering and Environmental Studies Program, Boston College, Chestnut Hill, MA 02467, USA
[46]National Centre for Earth Observation, School of Physics and Astronomy, University of Leicester, Leicester, LE1 7RH, UK
[47]Department of Biology Sciences, Institute of Environment Science, University of Quebec at Montreal, Montreal, QC H3C 3P8, Canada
[48] School of Geographic Sciences, Hunan Normal University, Changsha 410081, China
[49]Climate and Ecosystem Sciences Division, Lawrence Berkeley National Lab, 1 Cyclotron Road, Berkeley, CA 94720, US
[50]Department of Forest Ecology and Management, Swedish University of Agricultural Sciences, 90183 Umeå, Sweden
[51]Centre for Coastal Biogeochemistry, Faculty of Science and Engineering, Southern Cross University,

Lismore, NSW 2480, Australia
[52]TNO, dep. of Climate Air  Sustainability, P.O. Box 80015, NL-3508-TA, Utrecht, The Netherlands
[53]Joint Global Change Research Institute, Pacific Northwest National Lab, College Park, MD, USA
[54]Center for Global Sustainability, University of Maryland, College Park, MD, USA
[55]Center for Limnology, University of Wisconsin-Madison, Madison, WI, USA
[56]Empa, Swiss Federal Laboratories for Materials Science and Technology, Dübendorf, Switzerland
[57]Center for Earth System Science and Global Sustainability,Schiller Institute for Integrated Science and Society, Department of Earth and Environmental Sciences, Boston College, Chestnut Hill, MA 02467, USA
[58]Finnish Meteorological Institute, P.O. Box 503, FI-00101, Helsinki, Finland
[59]Statistics Division, Food and Agriculture Organization of the United Nations (FAO), Viale delle Terme di Caracalla, Rome 00153, Italy
[60]Department of Earth and Environmental Sciences, University of Rochester, Rochester, NY 14627, USA
[61]Meteorology and Air Quality Group, Wageningen University and Research, Wageningen, the Netherlands
[62]Environment and Climate Change Canada, 4905, Dufferin Street, Toronto, Canada
[63]Department of Physical Geography and Ecosystem Science, Lund University, Sölvegatan 12, 223 62, Lund, Sweden
[64]Institute of Environment and Ecology, Tsinghua Shenzhen International Graduate School, Tsinghua University, Shenzhen 518055, China ;
[65]State Environmental Protection Key Laboratory of Sources and Control of Air Pollution Complex, Beijing 100084, China
[66]College of Geography and Remote Sensing, Hohai University, Nanjing, 210098, China
*formerly at LSCE 1
April 29, 2024

## Contents

# List of Tables

# List of Figures

# 1 Comparisons with AR5 and AR6 projections

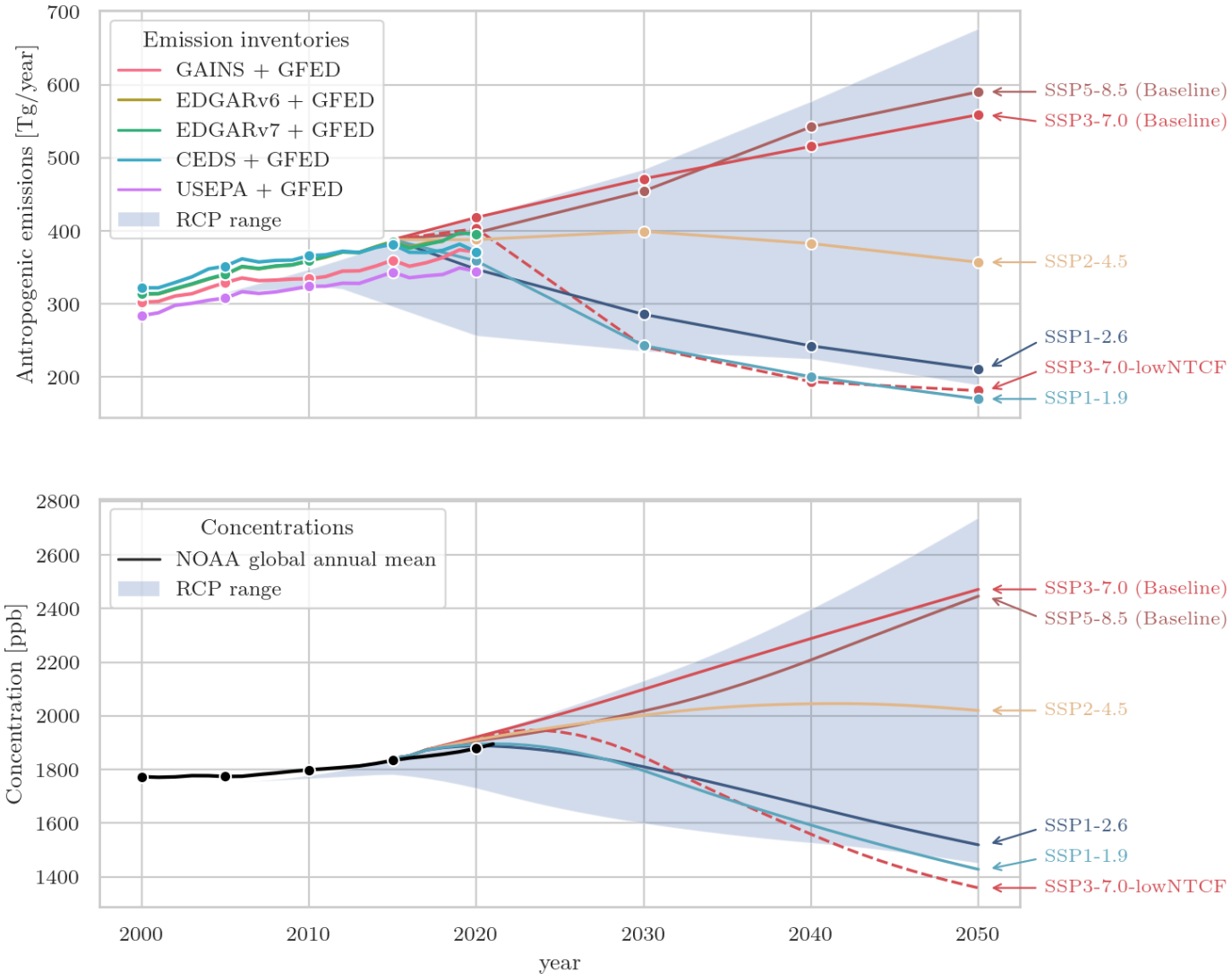


Figure S1: Time series of methane anthropogenic emissions (top) and atmospheric concentrations (bottom). RCPs (from AR5) and SSPs (from AR6) are shown on top of the anthropogenic total emission estimates from this study for emissions (top) and NOAA global mean atmospheric concentrations (bottom).

# 2 Supplementary text 1: Principle of inversions

An atmospheric inversion for methane fluxes (sources and sinks) optimally combines atmospheric observations of methane and associated uncertainties, a prior knowledge of the fluxes including their uncertainties, and a chemistry-transport model to relate fluxes to concentrations (Rodgers, 2000). In this sense, top-down inversions integrate all the components of the methane cycle described previously in this paper. The observations can be surface or upper-air in situ observations, satellite and surface retrievals. Prior emissions generally come from bottom-up approaches such as process-based models or data-driven extrapolations (natural sources) and inventories (anthropogenic sources). The chemistry-transport model can be Eulerian or Lagrangian, and global or regional, depending on the scale of the flux to be optimized. Atmospheric inversions generally rely on the Bayes theorem, which leads to the minimization of a cost function as Eq.1:

$$J(x) = \frac{1}{2}(y - H(x))^T R^{-1}(y - H(x)) + \frac{1}{2}(x - x_b)^T B^{-1}(x - x_b) \quad (1)$$

where y is a vector containing the atmospheric observations, x is a state vector containing the methane emissions and other appropriate variables (like OH concentrations or $CH_4$ concentrations at the start of the assimilation window) to be

estimated, $x_b$is the prior state of x, and H is the observation operator, here the combination of an atmospheric transport and chemistry model and an interpolation procedure sampling the model at the measurement coordinates. R is the error covariance matrix of the observations and $P_b$ is the error covariance matrix associated to. The errors on the modelling of atmospheric transport and chemistry are included in the R matrix (Tarantola, 1987). The minimization of a linearized version of J leads to the optimized state vector $x_a$ (Eq.2):

$$x_a = x_b + (H^T R^{-1} H + P_b^{-1})^{-1} H^T R^{-1} (y - H(x)) \tag{2}$$

where Pa is given by Eq.3 and represents the error covariance matrix associated to xa, and H contains the sensitivities of any observation to any component of state vector x (linearized version of the observation operator H(x)).

$$P_a = (H^T R^{-1} H + P_b^{-1})^{-1} \tag{3}$$

Unfortunately, the size of the inverse problem usually does not allow computing Pa, which is therefore approximated using the leading eigenvectors of the Hessian of J (Chevallier et al., 2005) or from stochastic ensembles (Chevallier et al., 2007). Therefore, the optimized fluxes $x_a$ are obtained using classical minimization algorithms (Chevallier et al., 2005; Meirink et al., 2008b). Alternatively, Chen and Prinn (2006) computed monthly emissions by applying a recursive Kalman filter in which Pa is computed explicitly for each month. Emissions are generally derived at weekly to monthly time scales, and for spatial resolutions ranging from model grid resolution to large aggregated regions. Spatio-temporal aggregation of state vector elements reduces the size of the inverse problem and allows the computation of $P_a$. However, such aggregation can also generate aggregation errors inducing possible biases in the inferred emissions and sinks (Kaminski et al., 2001). The estimated $x_a$ can represent either the net methane flux in a given region or contributions from specific source categories. Atmospheric inversions use bottom-up models and inventories as prior estimates of the emissions and sinks in their setup, which make B-U and T-D approaches generally not independent.

# 3 Supplementary text 2: Set of prior fluxes proposed by the atmospheric inversion protocol

A set of fluxes for the different methane sources has been gathered and made available to the community to perform atmospheric inversions.
We have used :

- biomass burning from GFED4.1s on a monthly basis up to 2020.
- the dynamical (monthly) wetlands emissions from the ensemble mean of 11 models contributing to the Global Methane Budget (Saunois et al. 2020)
- termite emissions from the model described in Saunois et al. (2020), representing a climatological estimate.
- emissions from oceans from Weber et al. (2019) geological emissions from Etiope et al. (2019) scaled to 23 Tg for global emission based on IPCC AR6 best estimates. This estimate is higher than Hmiel et al.(2020), but lower than Etiope et al., (2019). Offshore and onshore estimates were provided. We suggested to use only land emissions (onshore) to avoid double-counting offshore geological emissions with these from the "ocean" emission.
- the soils uptake is Saunois et al. (2020), based on Murgia-Flores et al. (2018).

We performed two rounds of inversions (v1 and v2).
The first round of inversions uses anthropogenic emissions from EDGARv6 database (Crippa et al., 2021; Oreggioni et al., 2021; EDGARv6 website `https://edgar.jrc.ec.europa.eu/dataset_ghg60`; Ferrario et al., 2021), which is available up to 2018.

For this study, the EDGARv6 was extrapolated up to 2019 using the FAO-CH4 emissions for CH4 emissions from enteric fermentation, manure management and rice cultivation, and using the BP statistical review of fossil fuel production and consumption (http://www.bp.com/) to update CH4 emissions from coal, oil and gas sectors. 2020 and 2021 emissions were set equal 2019 emissions.

Later, it was further extended to 2020 for the main budget. In this extrapolated inventory, called EDGARv6EXT, methane emissions for year t are set up equal to the 2018 EDGAR CH4 emissions (E_EDGARv6) times the ratio between the FAO-CH4 emissions (or BP statistics) of year t (E_FAO-CH4(t)) and FAO-CH4 emissions (or BP statistics) of 2018 (E_FAO-CH4(2018)). For each emission sector, the region-specific emissions (E_EDGARv6ext) in year (t) are estimated following Eq.4:

$$E_{EDGARv6}(t) = E_{EDGARv6}(2018) * E_{FAO-CH4}(t)/E_{FAO-CH4}(2018) \quad (4)$$

Transport, industrial, waste and biofuel sources were linearly extrapolated based on the last three years of data while other sources are kept constant at the 2018 level. This extrapolation approach is necessary, and often performed by top-down approaches to define prior emissions, because, up to now, global inventories such as sector-specific emissions in the EDGAR database are not updated on a regular basis.

A second round of inversion was performed by most of the groups using the GAINS gridded data set instead of EDGARv6 for all the fossil fuel related emissions. This was done due to a significant change on boreal emissions in EDGARv6 probably related to changes in data activity maps.

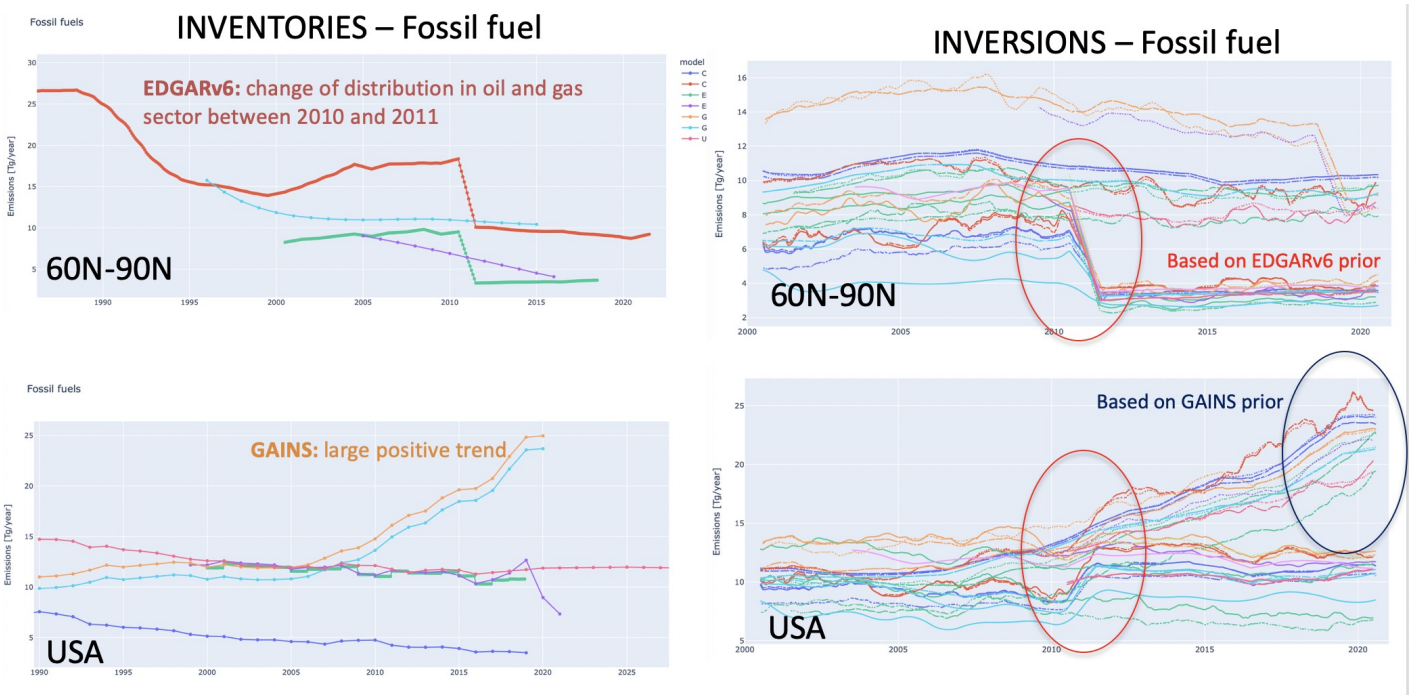


Figure S2: Emission in the fossil fuel sector in the inventories (left) and after data assimilation in inversions (right) for the boreal region (top) and the USA (bottom).

# 4 Definition of the regions

Figure S3: Map of the 18 continental regions.

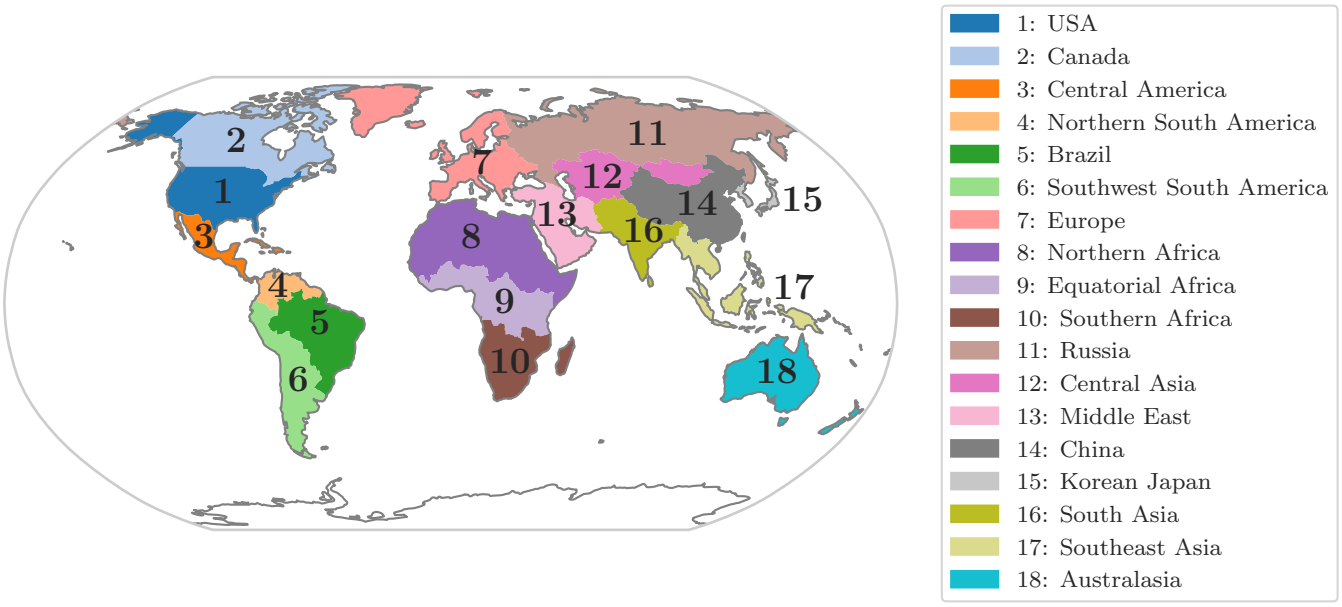

Table S1: List of the countries used to define the 18 continental regions. Compared to Saunois et al. (2020), regions are the same except for the last region includes only Australia and New-Zealand and is called *Australasia*.

| **N°** | **Region name** | **Countries or territories** |
|---|---|---|
| 1 | USA | USA with Alaska, Bermuda Islands |
| 2 | Canada | Canada |
| 3 | Central America | Anguilla, Antigua and Barbuda, Bahamas, Barbados, Belize, British Virgin Islands, Cayman Islands, Costa Rica, Cuba, Dominica, Dominican Republic, El Salvador, Guadeloupe, Guatemala, Honduras, Jamaica, Martinique, Mexico, Montserrat, Nicaragua, Panama, Puerto Rico, Saint Kitts and Nevis, Saint Lucia, Saint Vincent and the Grenadines, Turks and Caicos Islands, United States Virgin Islands |
| 4 | Brazil | Brazil |
| 5 | Northern South America | Aruba, Colombia, French Guiana, Grenada, Guyana, Suriname, Trinidad and Tobago, Venezuela |
| 6 | Southwest South America | Argentina, Bolivia, Chile, Ecuador, Peru, Falkland Islands (Malvinas), Paraguay, Uruguay |
| 7 | Europe | Albania, Andorra, Austria, Belarus, Belgium, Belgium, Luxembourg, Bulgaria, Channel Islands, Croatia, Cyprus, Czech Republic, Denmark, Estonia, Faroe Islands, Finland, France, Germany, Gibraltar, Greece, Greenland, Hungary, Iceland, Ireland, Isle of Man, Italy, Latvia, Liechtenstein, Lithuania, Luxembourg, Malta, Montenegro, Netherlands, Norway, Poland, Portugal, Republic of Moldova, Romania, Serbia, Slovakia, Slovenia, Spain, Sweden, United Kingdom, Ukraine |
| 8 | Northern Africa | Algeria, Cabo Verde, Chad, Côte d'Ivoire, Djibouti, Egypt, Eritrea, Ethiopia, Ethiopia PDR, Gambia, Guinea, Guinea-Bissau, Libya, Mali, Mauritania, Morocco, Saint Helena Ascension and Tristan da Cunha, Sao Tome and Principe, Senegal, Somalia, Sudan former, Tunisia, Western Sahara |
| 9 | Equatorial Africa | Benin, Burkina Faso, Burundi, Cameroon, Central African Republic, Congo, Democratic Republic of the Congo, Equatorial Guinea, Gabon, Ghana, Liberia, Nigeria, Rwanda, Sierra Leone, Togo, Uganda, United Republic of Tanzania |
| 10 | Southern Africa | Angola, Botswana, Comoros, Lesotho, Madagascar, Malawi, Mauritius, Mayotte, Mozambique, Namibia, Reunion, Seychelles, South Africa, Swaziland, Zambia, Zimbabwe |
| 11 | Russia | Russian federation |
| 12 | Central Asia | Kazakhstan, Kyrgyzstan, Tajikistan, Turkmenistan, Uzbekistan, Mongolia |
| 13 | Middle East | Armenia, Azerbaijan, Bahrain, People's Republic of Georgia, Iran, Iraq, Israel, Jordan, Kuwait, Lebanon, Occupied Palestinian Territory, Oman, Qatar, Saudi Arabia, Syrian Arab Republic, Turkey, United Arab Emirates, Yemen |
| 14 | China | China mainland, Macao, Hong Kong, Taiwan |
| 15 | Korea and Japan | Japan, Korea, Republic of Korea |
| 16 | South Asia | Afghanistan, Bangladesh, Bhutan, India, Nepal, Pakistan, Sri Lanka |
| 17 | South East Asia | American Samoa, Brunei Darussalam, Cambodia, Cook Islands, Fiji, French Polynesia, Guam, Indonesia, Kiribati, Lao People's Democratic Republic, Malaysia, Maldives, Marshall Islands, Myanmar, Nauru, New Caledonia, Niue, Norfolk Island, Northern Mariana Islands, Pacific Islands Trust Territory, Palau, Papua New Guinea, Pitcairn Islands, Philippines, Samoa, Singapore, Solomon Islands, Thailand, Timor-Leste, Tokelau, Tonga, Tuvalu, Vanuatu, Vietnam, Wallis and Futuna Islands |
| 18 | Australasia | Australia, New Zealand |

# 5 Tables and figures supporting the bottom-up-budget section

Table S2: Assignment of the inventory specific sectors to GCP sub and main categories

| | Category | EDGARv6.0 | GAINS by country | GAINS gridded | CEDS | USEPA |
|---|---|---|---|---|---|---|
| **Agriculture and Waste** | Enteric fermentation and Manure | ENF (Enteric fermentation)<br>MNM (Manure management) | Beef_cattle<br>Dairy_cows<br>Pigs<br>Other_livestock | agr_cow (cattle)<br>agr_buff (buffaloes)<br>agr_pig (pigs)<br>agr_gosh (sheep and goats)<br>agr_poult (poultry)<br>agr (other) | Agriculture (incl. Rice) | Livestock |
| | Rice cultivation | AGS (Agricultural soils) | Rice_cultivation | agr_fert (soils) | | Rice<br>OtherAg |
| | Landfills and Waste | SWD_LDF (Solid waste landfills)<br>SWD_INC (Solid waste incineration)<br>WWT (Waste water handling) | Solid_waste_industry<br>Solid_waste_municipal<br>Wastewater_industry<br>Wastewater_domestic | wst<br>wst_rur<br>wst_urb | Waste | Landfills<br>Wastewater<br>OtherWaste |
| **Fossil Fuels** | Oil & Gas | PRO_OIL (Fuel exploitation OIL)<br>PRO_GAS (Fuel exploitation GAS)<br>FFF (Fossil Fuel Fires) | Oil_production<br>Oil_refinery<br>Gas_production<br>Gas_distribution<br>Unconventional_gas_prod | flr_up (Oil and gas production) | Energy (incl. Coal) | NGO |
| | Coal | PRO_COAL (Fuel exploitation COAL) | Coal_mining<br>Abandoned_coal_mines | mbc (Coal mining)<br>mhc (Coal mining) | | Coal |
| | Industry | CHE (Chemical processes)<br>IRO (Iron and steel production)<br>ENE (Power industry)<br>IND (Combustion for manufacturing)<br>REF_TRF (Oil refineries and–<br>–Transformation industry) | Gas_transmission | ind (Industry)<br>pp_bio (Power plants -biofuel)<br>pp_coal (Power plants -coal)<br>pp_eng (Power engines)<br>pp_gas (Power plants -gas)<br>pp_oil (Power plants -oil) | Industrial<br>Solvents production–<br>–and application | OtherEnergy<br>OtherIPPU |
| | Transport | TRO_noRES (Road transportation no resuspension)<br>TNR_Aviation_CDS (Aviation climbing & descent)<br>TNR_Aviation_CRS (Aviation cruise)<br>TNR_Aviation_LTO (Aviation landing & takeoff)<br>TNR_Aviation_SPS (Aviation supersonic)<br>TNR_Other (Railways, pipelines, off-road transport)<br>TNR_Ship (Shipping) | Combustion_fossil_fuel | tra_rd_2w (2 wheelers)<br>tra_rd_hdb (Buses)<br>tra_rd_hdt (Trucks)<br>tra_rd_ld4 (Cars) | Transportation<br>International Shipping | Combustion (StatMob) |
| | Biofuels burning | RCO (Energy for buildings) | Combustion_biomass_fuel | dom_cook_r (Rural households)<br>dom_cook_u (Urban households)<br>dom_heat_r (Rural households) | Residential, Com–<br>–mercial, Other | Combustion (Biomass) |

Table S3: Contributions of the land surface models to compute methane wetland emissions to the different releases of the global methane budget.

| Model name | Kirschke et al. (2013) | Saunois et al. (2016)<br>Poulter et al. (2017) | Saunois et al. (2020) | This study |
|---|---|---|---|---|
| CH4MOD | – | – | – | Y |
| CLASS-CTEM // CLASSIC | – | Y | Y | Y |
| CLM4.5 | – | Y | – | – |
| DLEM | – | Y | Y | Y |
| ELM-ECA | – | – | Y | Y |
| ISAM | – | – | – | Y |
| JSBACH | – | – | Y | Y |
| JULES | – | Y | Y | Y |
| LPJ-GUESS | – | – | Y | Y |
| LPJ-MPI | – | Y | Y | Y |
| LPJ-wsl | Y | Y | Y | Y |
| LPX-Bern | Y | Y | Y | Y |
| ORCHIDEE | Y | Y | Y | Y |
| SDGVM | – | Y | – | Y |
| TEM-MDM | – | – | Y | Y |
| TRIPLEX-GHG | – | Y | Y | Y |
| VISIT | – | Y | Y | Y |
| **Contributing** | 3 | 11 | 13 | 16 |

Table S4: Tropospheric OH concentrations in $10^6$ molec cm$^{-3}$ and inter annual variability (IAV) in % from the ensemble of model contributing to CCMI-2022 (Plumer et al., 2021) and CMIP6 (Collins et al. (2021) modeling activities. Values are given as average values over the period 2000-2010 for CCMI-2020 and CMIP6 and for 2010-2018 for CMIP6 only.

| | mean [mil. molec/cm$^3$] | IAV [%] |
|---|---|---|
| CCMI2022 - 2000-2010 | | |
| ACCESS-CM2-Chem | 1.22 | 1.2 |
| CCSRNIES-MIROC32[b] | 2.37 | 2.4 |
| CMAM | 1.29 | 1.3 |
| CNRM-MOCAGE | 1.34 | 1.3 |
| EMAC-CCMI2 | 1.23 | 1.2 |
| GEOSCCM | 1.20 | 1.2 |
| IPSL-CM6A-ATM-LR-REPROBUS[a] | 0.17 | 0.2 |
| NIWA-UKCA2 | 1.17 | 1.2 |
| SOCOL | 1.82 | 1.8 |
| UKESM1-StratTrop | 1.39 | 1.4 |
| mean of 8 models [min-max] | 1.33 [1.17 - 1.82] | |
| CMIP6 - 2000-2010 | | |
| BCC-ESM1 | 0.79 | 0.8 |
| CESM2-FV2 | 1.20 | 1.2 |
| CESM2-WACCM-FV2 | 1.35 | 1.3 |
| CESM2-WACCM | 1.20 | 1.2 |
| CESM2 | 1.20 | 1.2 |
| CNRM-ESM2-1 [b] | 0.47 | 0.5 |
| EC-Earth3-AerChem | 1.20 | 1.2 |
| GISS-E2-1-G | 1.34 | 1.3 |
| GISS-E2-2-G | 1.26 | 1.3 |
| MPI-ESM-1-2-HAM | 0.97 | 1.0 |
| MRI-ESM2-0 | 0.94 | 0.9 |
| mean of 10 models [min-max] | 1.15 [0.79-1.35] | |
| CCMI2022 - 2010-2018 | | |
| ACCESS-CM2-Chem | 1.22 | 1.2 |
| CCSRNIES-MIROC32[b] | 2.38 | 2.4 |
| CMAM | 1.30 | 1.3 |
| CNRM-MOCAGE | 1.27 | 1.3 |
| EMAC-CCMI2 | 1.25 | 1.2 |
| GEOSCCM | 1.21 | 1.2 |
| IPSL-CM6A-ATM-LR-REPROBUS[a] | 0.17 | 0.2 |
| NIWA-UKCA2 | 1.17 | 1.2 |
| SOCOL | 1.85 | 1.9 |
| UKESM1-StratTrop | 1.40 | 1.4 |
| mean [min-max] of 8 models | 1.33 [1.17-1.85] | |

[a] no tropospheric chemical scheme in this model - removed from the ensemble
[b] outlier - removed from the ensemble

Table S5: Methane chemical loss in the troposphere[a] and stratosphere in Tg $yr^{-1}$ on average the decade 2000-2009 and 2010-2019 as calculated by chemistry climate models contributing CCMI-2022 (Plumer et al., 2021) and CMIP6 (Collins et al., 2021) modeling activities

| | Tropospheric loss | Stratospheric loss | Total chemical loss | Tropospheric lifetime[b] | Total lifetime[c] |
|---|---|---|---|---|---|
| CMIP6 (2000-2009) - Hist | | | | | |
| BCC-ESM1[d] | 794.3 | 27.2 | 821.5 | 6.2 | 5.7 |
| CESM2-WACCM | 663.3 | 39.9 | 703.2 | 7.5 | 6.8 |
| EC-Earth3-AerChem | 557.2 | 10.2 | 567.4 | 8.8 | 8.2 |
| GISS-E2-1-G | 527.7 | 51.2 | 578.9 | 9.3 | 8.1 |
| GISS-E2-1-H | 510.4 | 41.2 | 551.6 | 9.7 | 8.5 |
| MRI-ESM2-0 | 446.5 | 33.3 | 479.8 | 11.0 | 9.7 |
| mean [min-max] | 541 [446-663] | 35 [10-51] | 576 [480-703] | 9.3 [7.5-11.0] | 8.2 [6.8-9.7] |
| CCMI (2000-2009) | | | | | |
| BCC-ESM1[d] | 799.1 | 27.4 | 826.5 | 6.1 | 5.7 |
| CESM2-WACCM-FV2 | 606.8 | 38.1 | 644.9 | 8.1 | 7.3 |
| CESM2-WACCM | 650.9 | 39.3 | 690.2 | 7.6 | 6.9 |
| EC-Earth3-AerChem | 552.7 | 10.2 | 562.9 | 8.9 | 8.3 |
| GISS-E2-1-G | 487.6 | 41.2 | 528.8 | 10.1 | 8.8 |
| MRI-ESM2-0 | 452.3 | 32.8 | 485.1 | 10.9 | 9.5 |
| mean [min-max] | 550 [452-650] | 32 [10-39] | 582 [485-690] | 9.1 [7.7-10.9] | 8.2 [6.9-9.5] |
| Ensemble of 10 runs | | | | | |
| mean [min-max] | 546 [446-663] | 34 [10-51] | 579 [480-703] | 9.2 [7.5-11.0] | 8.2 [6.8-9.7] |
| CMIP6 (2010-2019) - Hist + SSP3-7.0 Starting in 2015 | | | | | |
| BCC-ESM1[d] | 836.6 | 27.8 | 864.4 | 6.0 | 5.6 |
| CESM2-WACCM | 693.4 | 40.9 | 734.3 | 7.4 | 6.7 |
| EC-Earth3-AerChem | 582.2 | 10.7 | 592.9 | 8.7 | 8.1 |
| GISS-E2-1-G | 540.8 | 43.3 | 584.1 | 9.4 | 8.3 |
| GISS-E2-1-H | 537.0 | 37.6 | 574.7 | 9.5 | 8.5 |
| MRI-ESM2-0 | 462.3 | 33.4 | 495.7 | 11.0 | 9.7 |
| mean [min-max] | 563 [462-663] | 33 [11-43] | 596 [496-734] | 9.2 [7.4-11.0] | 8.2 [6.7-9.7] |

[a] tropopause height at 200hPa
[b] defined as total burden divided by tropospheric loss
[c] defined as total burden divided by total loss. Total loss = total chemical loss (tropospheric and stratospheric losses) + 31 Tg from soil uptake for consistency with the main text budget. Note that changing the amount of soil uptake to 35 Tg will not change the results significantly (about 0.1 year).
[d] outlier regarding the tropospheric loss - removed from the ensemble

Table S6: Soil uptake estimates from the literature and in the Global Methane Budget in Tg $CH_4$ $yr^{-1}$

| Reference | Method | Period | Best estimate | Range | Range explanation |
|---|---|---|---|---|---|
| Ridgwell et al. (1999) | Modelling | 1990s | 38 | 20-51 | Model struct. uncertainty |
| Dutaur and Verchot (2007) | Extrapolation of obs. | ? | 22 | 10-34 | |
| Curry (2007) | Modelling- CLASS | 1979–1999 | 28 | 9-47 | |
| Riley et al. (2011) | Modeling - CLM4Me | ? | 31 | 15-38 | Struc. uncertainties |
| Ito and Inatomi (2012) | Modelling - VISIT | 1996-2005 | | 25-35 | |
| Tian et al. (2016) | Modelling - DLEM | 2000-2009 | 30 | 11-49 | |
| Murguia-Flores et al. (2018) | Modelling – MeMo | 2008-2017[a] | 32 | 29-38 | Different parametrizations |
| | Modelling – MeMo | 2000-2009[b] | 35 | 30-38 | Different parametrizations |
| | Modelling – MeMo | 2010-2019[b] | 36 | 31-39 | Different parametrizations |
| Kaiser et al. (2017) | Modelling – JSBACH | 2000-2009[b] | 17 | | |
| Kaiser et al. (2017) | Modelling – JSBACH | 2010-2019[b] | 18 | | |
| Ito and Inatomi et al. (2012) | Modelling – VISIT | 2000-2009[b] | 34 | | |
| Ito and Inatomi et al. (2012) | Modelling – VISIT | 2010-2019[b] | 37 | | |
| **Synthesis publications** | **Litterature based on** | | **Mean** | **Range** | |
| Kirschke et al. (2013) | Curry (2007) | | 28 | 9-47 | |
| Saunois et al. (2016) | Curry (2007) | | 28 | 9-47 | |
| Saunois et al. (2020) | Tian et al. (2016) | 2000-2009 | 30 | 11- 49 | |
| This study | | 2000-2009 | 31 | 17-39 | |
| This study | | 2010-2019 | 32 | 18-40 | |

[a] runs have been performed specifically for this period for Saunois et al. (2020)
[b] runs have been performed specifically for this period for this study

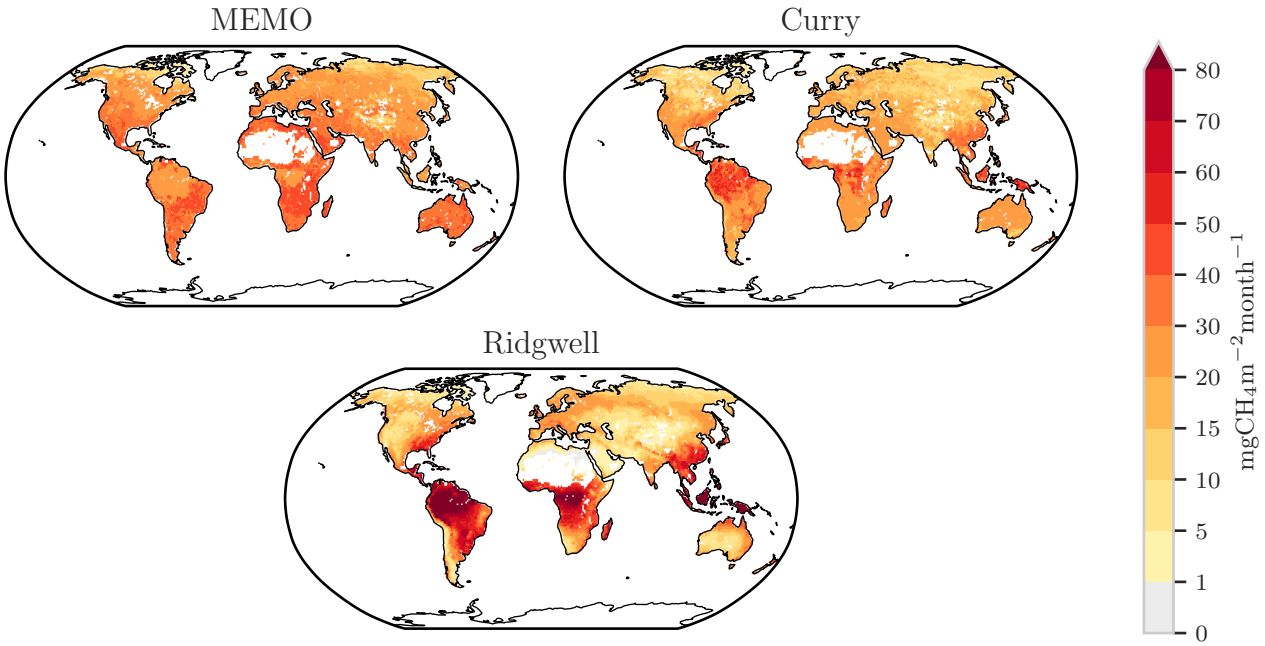


Figure S4: Distribution of the soil uptake from three different studies : MeMo (Murgia-Flores et al., 2018), Curry et al. (2007) and Ridgewell et al. (1999).

# 6 Table supporting the top-down budget section

Table S7: Contributions of the different inverse systems to the different releases of the global methane budget.

| Model name | Kirschke et al. (2013) | Saunois et al. (2016) | Saunois et al. (2020) | This study |
|---|---|---|---|---|
| CTE-CH4 (NOAA) | Surface | Surface | – | – |
| CTE-CH4 (FMI) | – | – | Surface/GOSAT | Surface |
| GELCA | – | Surface | Surface | – |
| GEOSCHEM | Surface | – | – | – |
| GISS | Surface | – | – | – |
| LMDz-CIF | – | – | – | Surface |
| LMDz-MIOP | Surface | Surface | – | – |
| LMDz-PYVAR | Surface | Surface/GOSAT | Surface/GOSAT | GOSAT |
| MATCH | Surface | – | – | – |
| MIROC4-ACTM | – | Surface | Surface | Surface |
| NICAM-TM | – | – | Surface | Surface |
| NIESTM | – | Surface/GOSAT | Surface/GOSAT | Surface/GOSAT |
| TM2 | Surface | – | – | – |
| TM5-CAMS (TM5-SRON) | Surface | Surface/GOSAT | Surface/GOSAT | Surface/GOSAT |
| TM5-JRC | Surface | Surface/GOSAT | Surface/GOSAT | – |
| TOMCAT | – | – | Surface | – |
| **Contributing** | 9 | 8 | 9 | 7 |

Table S8: Characteristics of the top-down inverse systems contributing to this study. CTE-CH4, LMDz- CIF, abd LMDz-PYVAR. 1/2

| | | CTE-CH4 | LMDz- CIF | LMDz-PYVAR |
|---|---|---|---|---|
| Main ref. | | Tsuruta et al. (2017) | Thanwerdas et al. (2022) | Zheng et al. (2018a, 2018b) |
| Model Characteristics | Meteorology | ECMWF ERA5 | LMDz nudged to ERA-I | LMDz nudged to ERA5 |
| | Resolution | Global 6x4 + two-way nested 1x1 zoom over Europe, 25 levels | (3.75° longitude × 1.9° latitude × 39 layers) | (3.75° longitude × 1.9° latitude × 39 layers) |
| | PBL scheme | Based on parameterisation of Vogelezang and Holtslag (1996) (Krol et al., 2018) | ECMWF ERA-Interim 6 hourly PBL height | ECMWF ERA5 6 hourly PBL height |
| | Convection Scheme | Gregory et al., 2000 | Tiedtke's scheme | Tiedtke's scheme |
| Inversion set-up | Time resolution | 1 week | 8 days | 8 days |
| | Spatial resolution | 1x1 over Europe, Russia, USA and Canada. Region-wise elsewhere | 3.75° longitude × 1.9° latitude | 3.75° longitude × 1.9° latitude |
| | Prior errors | 80% of flux over land, 20% over ocean | 70% of prior emissions | 70% of prior emissions |
| | Correlation length | 100 km over 1x1 region, 500 km over other land regions, 900 km over ocean | 1000 km (ocean), 500 km (land), 16 days (temporal) | 1000 km (ocean), 500 km (land), 16 days (temporal) |
| | Minimizers | Ensemble Kalman filter (Peters et al., 2005) | M1QN3 | M1QN3 |
| | Control vector (temporal and sectorial resolution) | 1 week, 2 categories: anthropogenic + biomass burning + rice, wetlands + soil uptake | 10 days, 12 emission fluxes categories, 3.75° longitude × 1.9° latitude | 8 days, total emission fluxes, 3.75° longitude × 1.9° latitude |
| Prior sources | Anthropogenic | GCP | GCP | GCP |
| | Biomass burning | GCP | GCP | GCP |
| | Wetlands | GCP | GCP | GCP |
| | Rice | GCP | GCP | GCP |

Table S9: Characteristics of the top-down inverse systems contributing to this study. CTE-CH4, LMDz- CIF, abd LMDz-PYVAR. 2/2

| | | CTE-CH4 | LMDz- CIF | LMDz-PYVAR |
|---|---|---|---|---|
| Prior Sources | Termites | GCP | GCP | GCP |
| | Other | GCP (geological and oceans) | GCP (geological and oceans) | GCP (geological and oceans) |
| Prior sinks | Soil uptake | GCP | GCP | GCP |
| | Chemistry | OH, O1D, Cl Transcom-CH4 (Patra et al., 2011) | OH, O1D Transcom-CH4 (Patra et al., 2011) | OH, O1D Transcom-CH4 (Patra et al., 2011) |
| Assimilated Data | Surface Obs. | AGAGE, CSIRO, EC, FMI, LSCE, NIES, NOAA, (part of) WDCGG, MPI-BGC, University of Exeter | AGAGE, CSIRO, EC, FMI, LSCE, NIES, NOAA, (part of) WDCGG, MPI-BGC, University of Exeter | |
| | Satellite data | | - | GOSAT University of Leicester v9.0 |
| | Satellite data processing if any | | - | |
| Observation errors | Surface observation | 4.5 to 75 ppb, depending on sites. No spatial/temporal correlation. | 4.5 to 75 ppb, depending on sites. No spatial/temporal correlation. | - |
| | Satellite Data | | - | Grid dependent. 150-200 ppb that includes instrument, representation, and forward model errors. |
| Time window | | 1 week | June 1999- June 2021 | 24 months each year (Jul-Jun) |
| Time period covered | | 2000-2020 | Surface : 2000-2020 | Satellite: 2010-2020 |

Table S10: Characteristics of the top-down inverse systems contributing to this study. MIROC4-ACTM, NIESMON-CH4, NIES-TM-FLEXPART, and TM5-CAMS. 1/2

| | | MIROC4-ACTM | NIESMON-CH4 | NIES-TM-FLEXPART | TM5-CAMS |
|---|---|---|---|---|---|
| Main ref. | | Patra et al. (2018); Watanabe et al. (2008) | Niwa et al. (2022) | Maksyutov et al. (2020); Wang (2019a) | Segers et al. (2022, report); Bergamaschi et al. (2010; 2013), Panday et al. (2016) |
| Model Characteristics | Meteorology | JRA-55 (Kobayashi et al., 2015) | JRA-55 (Kobayashi et al., 2015; Harada et al., 2016) | JCDAS/JRA-55 (FLEXPART), ERA5 (NIES-TM) | ECMWF ERA-Interim, forecasts 3-12 hour, 3 hourly temporal resolution |
| | Resolution | 2.8 x 2.8 x 67 | 223 km, 40 levels (model top 45km) | 3.75° × 3.75° × 42 levels NIES-TM, 0.1° × 0.1° FLEXPART | 3 x 2 x 34 |
| | PBL scheme | Mellor and Yamada (1974, 1982) | Mellor and Yamada (1974) & Nakanishi and Niino (2004) | ERA5 turbulent diffusion | LTG (Louis, Tiedtke and Geleyn) following Holtslag and Boville (1993) |
| | Convection Scheme | Arakawa and Schubert (1974) | Chikira and Sugiyama (2010) | ERA5 convective mass fluxes | ERA-Interim archived convective fluxes |
| Inversion set-up | Time resolution | Monthly | monthly | 15 days | Monthly |
| | Spatial resolution | 2.8 x 2.8 | 1° × 1° | 0.1° × 0.1° | 3 x 2 x 34 |
| | Prior errors | 50% of the fluxes over all the basis regions | calculated from the ensemble of VISIT for wetlands, rice cultivation, and soil uptake, and set 30 % for the others | EDGAR 6.0 for anthropogenic (30% of prior, each category), and GCP wetlands (50% of prior) emissions | 100% for categories wetlands, rice, and biomass burning; 50% for category with remaining sources (mainly anthropogenic) |
| | Correlation length | 0 between all the basis regions | calculated from the ensemble of VISIT for wetlands, rice cultivation, and soil uptake, and set 0 km for coal, oil &gas, biomass burnings, and set 500 km for the others | 500 km (spatial), 15 days (temporal) | 500 km |
| | Minimizers | Bayesian method | POpULar (Fujii and Kamachi, 2003; Fujii, 2005) | M1QN3 | M1QN3 |
| | Control vector (temporal and sectorial resolution) | | annual for 5 categories (anthropogenic emisssions except rice cultivation), monthly for 4 categories (fire, wetland, rice, and soil uptake), climatology for 1 category (termite+geological+ocean) | 0.2° × 0.2°, 15 days, 6 categories: gas, coal, agriculture, biofuel, waste, wetlands | |

Table S11: Characteristics of the top-down inverse systems contributing to this study. MIROC4-ACTM, NIESMON-CH4, NIES-TM-FLEXPART, and TM5-CAMS. 2/2

| | | MIROC4-ACTM | NIESMON-CH4 | NIES-TM-FLEXPART | TM5-CAMS |
|---|---|---|---|---|---|
| Prior sources | Anthropogenic | | GCP | GCP | |
| | Biomass burn. | | GCP | GCP | |
| | Wetlands | | GCP | GCP | |
| | Rice | | GCP | GCP | |
| | Termites | | GCP | GCP | |
| | Other | | GCP (geological and oceans) | GCP (geological and oceans) | |
| Prior sinks | Soil uptake | | GCP | GCP | |
| | Chemistry | | OH, O1D, Cl Transcom-CH4 (Patra et al., 2011) | OH, O1D, Cl Transcom-CH4 (Patra et al., 2011) | |
| Data assimilated | Surface Obs. | NOAA, CSIRO (41 stations) | All data in obspack_ch4_1_GLOBALVIEWplus_v4.0_2021-10-14 (Schuldt et al., 2021), and obspack_ch4_1_NRT_v4.0_2022-03-03 (Schuldt et al., 2021), and additional NIES data (JR-station, HAT, COI, CLA, DMV, NTL, HPP, VOS, MFJ, Mirai) | Obspack, ICOS, "background" sites with max 34 ppb RMSE | NOAA |
| | Satellite Data | - | - | GOSAT NIES L2 retrieval v02.95 (Yoshida et al., 2013) | GOSAT ESA/CCI product v2.3.8 (Detmers & Hasekamp, 2016, report |
| | Satellite data processing if any | - | - | bias correction varying by 5 deg latitude band and month | Latitudinal bias correction applied based on the biases between posterior TM5 simulations from the in-situ inversion and the GOSAT product. |
| Observation errors | Surface observation | Variable model error + 5ppb instrumental error | variable error according to simulated or observed monthly std with deweighting according to the number of observations within a 500 km-radius circle | 10 to 44 ppb, depending on sites | Following Bergamaschi et al. (2010) |
| | Satellite Data | - | - | 60 ppb | Combination of GOSAT retrieval and model representation errors. |
| Time window | | Monthly | 261 months (Jul 1999 – Mar 2021) | 18 month each year (Oct-Mar) | Sequence of 3 yearly inversions (2000-2014) or 1 yearly (2015, 2016,2017) , each with 6 months spin-up/spin-down. |
| Time period covered | | 2000-2020 | 2000-2020 | Surface : 2000-2020<br>Satellite: 2010-2020 | Surface : 2000-2020<br>Satellite: 2010-2020 |

# 7 Comparison of 2000-2009 decadal emissions through the different budgets

Table S12: Global methane emissions by source type for 2000 - 2009 decade ($TgCH_4\,yr^{-1}$)

| | Saunois et al. (2016) | | Saunois et al. (2020) | | This work | |
|---|---|---|---|---|---|---|
| Approach | Bottom-up | Top-down | Bottom-up | Top-down | Bottom-up | Top-down |
| Natural sources | | | | | | |
| Wetlands | 183 [151-222] | 166 [125-204] | 147 [102-179] | 180 [153-196] | 153 [116-189] | 158 [145-172] |
| Freshwaters | 122 [60-180] | | 209 [134-284] | | 89 [40-166] | |
| Other natural sources | 199 [104-297] | 68 [21-130] | 222 [143-306] | 35 [21-47] | 63 [24-93] | 44 [40-46] |
| Geological | 40 [30-56] | | 38 [13-53] | | 35 [13-53] | 22 [21-25] |
| Termites | 9 [3-15] | | 9 [3-15] | | 10 [4-16] | 10 [9-11] |
| Oceanic sources | 14 [5-25] | | 13 [9-22] | | 13 [6-20] | 12 [11-12] |
| Total natural sources | 382 [255-519] | 234 [194-292] | 369 [245-485] | 215 [176-243] | 216 [140-282] | 204 [189-223] |
| Anthropogenic sources | | | | | | |
| Agriculture and waste | 189 [169-205] | 183 [112-241] | 192 [171-206] | 202 [198-219] | 195 [175-215] | 210 [197-223] |
| Enteric ferm. & manure | 103 [95-109] | | 104 [93-109] | | 104 [100-110] | 108 [108-108] |
| Landfills & waste | 57 [51-61] | | 60 [55-63] | | 61 [52-71] | 65 [62-71] |
| Rice cultivation | 29 [23-35] | | 28 [23-34] | | 30 [24-34] | 35 [34-35] |
| Fossil fuels | 112 [107-126] | 101 [77-126] | 110 [94-129] | 101 [71-151] | 105 [97-123] | 105 [88-115] |
| Coal mining | 36 [24-43] | | 32 [24-42] | | 30 [26-32] | 29 [24-32] |
| Oil & gas | 76 [64-85] | | 73 [60-85] | | 65 [63-71] | 77 [64-90] |
| Industry | | | 2 [0-6] | | 4 [1-8] | |
| Transport | | | 4 [1-11] | | 3 [1-8] | |
| Biomass & biofuel burning | 30 [26-34] | 35 [16-53] | 31 [26-46] | 29 [23-35] | 30 [22-44] | 26 [22-29] |
| Biomass burning | 18 [15-20] | | 19 [15-32] | | 19 [14-29] | 14 [11-16] |
| Biofuel burning | 12 [9-14] | | 12 [9-14] | | 11 [8-14] | 11 [6-12] |
| Total anthropogenic sources | 338 [329-342] | 319 [255-357] | 334 [321-358] | 332 [312-347] | 333 [305-365] | 341 [319-355] |
| Sinks | | | | | | |
| Total chemical loss | 604 [483-738] | 514 | 595 [489-749] | 505 [459-516] | | 504 [496-511] |
| Tropospheric OH | 528 [454-617] | | 553 [476-677] | | | 472 [468-477] |
| Stratospheric loss | 51 [16-84] | | 31 [12-37] | | | 27 [23-36] |
| Tropospheric Cl | 25 [13-37] | | 32 [27-38] | | | 3 [0-8] |
| Soil uptake | 28 [9-47] | 32 [27-38] | 30 [11-49] | 34 [27-41] | 35 [30-38] | 34 [34-34] |
| Total sinks | 632 [492-785] | 546 | 625 [500-798] | 539 [486-557] | | 538 [530-545] |
| Sources - sink imbalance | | | | | | |
| Total sources | 720 [584-861] | 552 [535-566] | 703 [566-843] | 547 [524-560] | 549 [445-647] | 543 [526-558] |

# 8 Regional budgets: Tables and plots

Table S13: USA, Canada, Central America methane emissions by source type ($TgCH_4\,yr^{-1}$)

| Region | USA | | Canada | | Central America | |
|---|---|---|---|---|---|---|
| Approach | Bottom-up | Top-down | Bottom-up | Top-down | Bottom-up | Top-down |
| Natural sources | | | | | | |
| Comb. wetland & inland freshwaters | 16 [4-30] | 5 [5-6] | 30 [10-60] | 12 [9-18] | 6 [2-14] | 4 [4-5] |
| Wetlands | 10 [2-19] | | 14 [3-26] | | 4 [1-9] | |
| Freshwaters | 6 [3-12] | | 17 [7-34] | | 2 [1-5] | |
| Other natural sources | 8 [3-12] | 5 [3-7] | 2 [1-3] | 1 [1-1] | 2 [1-3] | 1 [1-2] |
| Total natural sources | 24 [7-43] | 12 [7-22] | 32 [11-63] | 14 [11-22] | 8 [3-17] | 5 [2-6] |
| Anthropogenic sources | | | | | | |
| Agriculture and waste | 14 [12-16] | 13 [9-16] | 2 [2-3] | 2 [1-3] | 7 [6-9] | 9 [8-10] |
| Enteric ferm. & manure | 9 [7-9] | | 1 [1-1] | | 4 [3-5] | |
| Landfills & waste | 5 [4-6] | | 1 [1-1] | | 3 [2-4] | |
| Rice cultivation | 0 [0-1] | | 0 [0-0] | | 0 [0-0] | |
| Fossil fuels | 11 [4-18] | 12 [7-16] | 3 [1-4] | 4 [2-5] | 2 [1-3] | 2 [2-3] |
| Coal mining | 3 [2-3] | | 0 [0-0] | | 0 [0-0] | |
| Oil & gas | 8 [1-12] | | 2 [1-4] | | 1 [1-2] | |
| Industry | 0 [0-1] | | 0 [0-0] | | 0 [0-0] | |
| Transport | 0 [0-1] | | 0 [0-0] | | 0 [0-0] | |
| Biomass & biofuel burning | 1 [0-1] | 1 [0-1] | 1 [0-1] | 1 [0-1] | 1 [0-1] | 0 [0-1] |
| Biomass burning | 0 [0-0] | | 1 [0-1] | | 0 [0-0] | |
| Biofuel burning | 0 [0-0] | | 0 [0-0] | | 0 [0-0] | |
| Total anthropogenic sources | 26 [19-34] | 25 [16-31] | 6 [3-8] | 7 [5-9] | 10 [8-12] | 12 [11-13] |
| Total sources | 49 [27-77] | 38 [32-46] | 38 [14-71] | 20 [17-24] | 18 [10-28] | 17 [14-19] |

Table S14: Northern South America, Brazil, Southwest South America methane emissions by source type ($TgCH_4\,yr^{-1}$)

| Region | Northern South America | | Brazil | | Southwest South America | |
|---|---|---|---|---|---|---|
| Approach | Bottom-up | Top-down | Bottom-up | Top-down | Bottom-up | Top-down |
| Natural sources | | | | | | |
| Comb. wetland & inland freshwaters | 8 [2-15] | 8 [6-10] | 29 [10-52] | 24 [20-33] | 18 [5-31] | 22 [14-33] |
| Wetlands | 7 [2-11] | | 25 [8-41] | | 14 [3-21] | |
| Freshwaters | 1 [0-3] | | 5 [2-11] | | 4 [1-9] | |
| Other natural sources | 2 [1-3] | 1 [1-2] | 3 [1-4] | 2 [2-3] | 3 [1-4] | 2 [2-3] |
| Total natural sources | 10 [3-17] | 9 [7-11] | 32 [11-57] | 26 [22-36] | 21 [6-35] | 24 [16-34] |
| Anthropogenic sources | | | | | | |
| Agriculture and waste | 4 [3-4] | 4 [4-5] | 16 [14-19] | 19 [14-22] | 10 [8-12] | 12 [9-14] |
| Enteric ferm. & manure | 3 [3-3] | | 12 [11-13] | | 7 [6-9] | |
| Landfills & waste | 1 [0-1] | | 3 [3-5] | | 2 [1-2] | |
| Rice cultivation | 0 [0-0] | | 0 [0-1] | | 0 [0-0] | |
| Fossil fuels | 5 [2-13] | 2 [2-3] | 1 [0-1] | 1 [0-2] | 2 [1-3] | 2 [1-2] |
| Coal mining | 0 [0-1] | | 0 [0-0] | | 0 [0-0] | |
| Oil & gas | 2 [1-2] | | 0 [0-1] | | 1 [1-2] | |
| Industry | 0 [0-0] | | 0 [0-1] | | 0 [0-0] | |
| Transport | 0 [0-0] | | 0 [0-0] | | 0 [0-0] | |
| Biomass & biofuel burning | 0 [0-0] | 0 [0-0] | 1 [1-2] | 1 [1-2] | 1 [1-1] | 1 [1-1] |
| Biomass burning | 0 [0-0] | | 1 [1-1] | | 1 [1-1] | |
| Biofuel burning | 0 [0-0] | | 0 [0-0] | | 0 [0-0] | |
| Total anthropogenic sources | 9 [6-17] | 7 [6-8] | 19 [16-22] | 21 [17-26] | 13 [10-16] | 14 [12-17] |
| Total sources | 19 [9-35] | 16 [13-20] | 51 [26-79] | 47 [41-58] | 34 [16-51] | 38 [30-48] |

Table S15: Europe, Northern Africa, Equatorial Africa methane emissions by source type ($TgCH_4\,yr^{-1}$)

| Region | Europe | | Northern Africa | | Equatorial Africa | |
|---|---|---|---|---|---|---|
| Approach | Bottom-up | Top-down | Bottom-up | Top-down | Bottom-up | Top-down |
| Natural sources | | | | | | |
| Comb. wetland & inland freshwaters | 9 [3-17] | 2 [2-2] | 6 [2-11] | 5 [4-7] | 21 [9-45] | 22 [19-28] |
| Wetlands | 5 [1-9] | | 2 [0-4] | | 14 [6-31] | |
| Freshwaters | 4 [2-8] | | 3 [1-7] | | 7 [3-15] | |
| Other natural sources | 8 [3-13] | 6 [3-7] | 1 [0-2] | 1 [1-1] | 2 [1-3] | 2 [1-2] |
| Total natural sources | 17 [6-30] | 7 [5-9] | 7 [2-13] | 6 [6-8] | 23 [10-49] | 24 [20-30] |
| Anthropogenic sources | | | | | | |
| Agriculture and waste | 19 [17-23] | 19 [16-23] | 11 [4-15] | 13 [12-14] | 11 [7-15] | 13 [11-15] |
| Enteric ferm. & manure | 11 [10-12] | | 7 [2-10] | | 6 [5-7] | |
| Landfills & waste | 8 [6-12] | | 3 [2-4] | | 3 [2-4] | |
| Rice cultivation | 0 [0-0] | | 0 [0-1] | | 2 [1-3] | |
| Fossil fuels | 5 [3-6] | 4 [2-7] | 6 [5-7] | 5 [4-7] | 7 [4-8] | 6 [3-10] |
| Coal mining | 2 [1-2] | | 0 [0-0] | | 0 [0-0] | |
| Oil & gas | 2 [0-4] | | 5 [4-5] | | 5 [2-8] | |
| Industry | 0 [0-1] | | 0 [0-1] | | 0 [0-2] | |
| Transport | 0 [0-0] | | 0 [0-0] | | 0 [0-0] | |
| Biomass & biofuel burning | 1 [0-1] | 1 [1-1] | 1 [0-2] | 1 [1-1] | 5 [3-8] | 5 [4-5] |
| Biomass burning | 0 [0-0] | | 0 [0-1] | | 2 [2-3] | |
| Biofuel burning | 1 [0-1] | | 1 [1-1] | | 2 [2-2] | |
| Total anthropogenic sources | 25 [22-27] | 24 [20-31] | 18 [16-20] | 19 [17-21] | 24 [19-34] | 23 [19-29] |
| Total sources | 42 [29-57] | 31 [24-36] | 24 [18-33] | 25 [23-29] | 47 [28-83] | 47 [39-59] |

Table S16: Southern Africa, Russia, Central Asia methane emissions by source type ($TgCH_4\,yr^{-1}$)

| Region | Southern Africa | | Russia | | Central Asia | |
|---|---|---|---|---|---|---|
| Approach | Bottom-up | Top-down | Bottom-up | Top-down | Bottom-up | Top-down |
| Natural sources | | | | | | |
| Comb. wetland & inland freshwaters | 10 [2-27] | 7 [4-9] | 22 [7-41] | 11 [8-13] | 7 [2-19] | 1 [1-1] |
| Wetlands | 6 [-0-18] | | 13 [4-23] | | 0 [-0-2] | |
| Freshwaters | 4 [2-9] | | 9 [4-18] | | 7 [2-17] | |
| Other natural sources | 1 [1-2] | 1 [1-1] | 4 [2-6] | 3 [1-4] | 1 [0-1] | 1 [0-1] |
| Total natural sources | 11 [2-29] | 8 [7-10] | 25 [9-47] | 14 [11-18] | 8 [2-19] | 1 [0-2] |
| Anthropogenic sources | | | | | | |
| Agriculture and waste | 5 [1-8] | 5 [4-6] | 5 [5-6] | 5 [3-6] | 3 [2-3] | 3 [2-5] |
| Enteric ferm. & manure | 2 [1-3] | | 2 [2-2] | | 2 [1-3] | |
| Landfills & waste | 2 [0-5] | | 3 [3-4] | | 1 [0-1] | |
| Rice cultivation | 0 [0-0] | | 0 [0-0] | | 0 [0-0] | |
| Fossil fuels | 3 [1-4] | 4 [3-4] | 15 [9-27] | 14 [8-23] | 5 [3-6] | 5 [4-7] |
| Coal mining | 1 [0-2] | | 3 [2-4] | | 1 [1-1] | |
| Oil & gas | 1 [0-3] | | 12 [6-24] | | 3 [1-5] | |
| Industry | 0 [0-1] | | 0 [0-2] | | 0 [0-0] | |
| Transport | 0 [0-0] | | 0 [0-0] | | 0 [0-0] | |
| Biomass & biofuel burning | 3 [1-4] | 3 [2-3] | 2 [1-4] | 2 [1-2] | 0 [0-0] | 0 [0-0] |
| Biomass burning | 2 [1-3] | | 1 [1-3] | | 0 [0-0] | |
| Biofuel burning | 0 [0-1] | | 0 [0-0] | | 0 [0-0] | |
| Total anthropogenic sources | 10 [3-14] | 11 [10-12] | 23 [15-36] | 21 [14-29] | 8 [4-10] | 9 [7-11] |
| Total sources | 21 [5-43] | 19 [16-24] | 48 [24-83] | 36 [27-45] | 15 [6-29] | 10 [8-13] |

Table S17: Middle East, China, Korean Japan methane emissions by source type ($TgCH_4\,yr^{-1}$)

| Region | Middle East | | China | | Korean Japan | |
|---|---|---|---|---|---|---|
| Approach | Bottom-up | Top-down | Bottom-up | Top-down | Bottom-up | Top-down |
| Natural sources | | | | | | |
| Comb. wetland & inland freshwaters | 4 [1-8] | 1 [0-1] | 12 [3-30] | 3 [2-4] | 1 [0-5] | 0 [0-1] |
| Wetlands | 1 [0-1] | | 7 [1-18] | | 1 [0-4] | |
| Freshwaters | 3 [1-7] | | 5 [2-12] | | 0 [0-1] | |
| Other natural sources | 5 [2-7] | 3 [1-5] | 2 [1-4] | 1 [0-2] | 1 [0-2] | 1 [1-1] |
| Total natural sources | 9 [3-15] | 4 [1-6] | 15 [4-33] | 4 [3-7] | 3 [1-7] | 1 [1-1] |
| Anthropogenic sources | | | | | | |
| Agriculture and waste | 9 [7-10] | 10 [9-11] | 32 [19-44] | 30 [13-36] | 3 [2-4] | 4 [3-4] |
| Enteric ferm. & manure | 3 [2-4] | | 11 [8-16] | | 1 [1-1] | |
| Landfills & waste | 5 [4-6] | | 11 [6-14] | | 1 [1-1] | |
| Rice cultivation | 0 [0-0] | | 9 [5-14] | | 1 [1-1] | |
| Fossil fuels | 17 [9-21] | | 24 [23-26] | | 1 [0-1] | |
| Coal mining | 0 [0-0] | | 21 [20-21] | | 0 [0-1] | |
| Oil & gas | 16 [8-20] | | 2 [2-2] | | 0 [0-0] | |
| Industry | 0 [0-0] | | 1 [0-1] | | 0 [0-0] | |
| Transport | 0 [0-0] | | 0 [0-1] | | 0 [0-0] | |
| Biomass & biofuel burning | 0 [0-0] | 0 [0-0] | 2 [1-4] | 3 [0-4] | 0 [0-0] | 0 [0-0] |
| Biomass burning | 0 [0-0] | | 0 [0-1] | | 0 [0-0] | |
| Biofuel burning | 0 [0-0] | | 2 [1-3] | | 0 [0-0] | |
| Total anthropogenic sources | 26 [18-31] | 28 [20-34] | 57 [51-66] | 53 [34-66] | 4 [3-5] | 4 [3-5] |
| Total sources | 35 [21-47] | 31 [24-39] | 71 [55-99] | 57 [37-72] | 6 [4-12] | 5 [4-6] |

Table S18: South Asia, Southeast Asia, Australasia methane emissions by source type ($TgCH_4\,yr^{-1}$)

| Region | South Asia | | Southeast Asia | | Australasia | |
|---|---|---|---|---|---|---|
| Approach | Bottom-up | Top-down | Bottom-up | Top-down | Bottom-up | Top-down |
| Natural sources | | | | | | |
| Comb. wetland & inland freshwaters | 12 [5-23] | 5 [4-6] | 27 [17-45] | 24 [14-29] | 7 [3-15] | 4 [4-5] |
| Wetlands | 9 [3-17] | | 24 [16-38] | | 3 [1-6] | |
| Freshwaters | 3 [1-6] | | 3 [1-7] | | 4 [2-9] | |
| Other natural sources | 1 [0-2] | 1 [1-1] | 6 [2-9] | 4 [2-6] | 3 [1-4] | 2 [2-2] |
| Total natural sources | 13 [5-25] | 6 [5-6] | 32 [19-54] | 27 [20-34] | 10 [4-19] | 6 [4-7] |
| Anthropogenic sources | | | | | | |
| Agriculture and waste | 37 [26-45] | 39 [33-43] | 19 [14-25] | 24 [21-31] | 5 [4-5] | 4 [4-5] |
| Enteric ferm. & manure | 20 [18-22] | | 4 [3-5] | | 4 [3-4] | |
| Landfills & waste | 9 [4-11] | | 6 [4-8] | | 1 [1-1] | |
| Rice cultivation | 8 [5-12] | | 9 [8-12] | | 0 [0-0] | |
| Fossil fuels | 4 [4-5] | 4 [3-4] | 8 [5-10] | 8 [6-11] | 2 [1-2] | 2 [1-2] |
| Coal mining | 2 [1-3] | | 5 [4-5] | | 1 [1-1] | |
| Oil & gas | 1 [1-2] | | 3 [1-4] | | 0 [0-0] | |
| Industry | 0 [0-1] | | 0 [0-1] | | 0 [0-0] | |
| Transport | 0 [0-0] | | 0 [0-0] | | 0 [0-0] | |
| Biomass & biofuel burning | 3 [2-3] | 2 [2-3] | 5 [2-7] | 4 [2-5] | 1 [0-1] | 1 [0-1] |
| Biomass burning | 0 [0-1] | | 4 [1-6] | | 1 [0-1] | |
| Biofuel burning | 2 [2-3] | | 1 [0-1] | | 0 [0-0] | |
| Total anthropogenic sources | 45 [44-47] | 45 [38-49] | 32 [23-39] | 35 [31-46] | 7 [6-7] | 7 [6-7] |
| Total sources | 58 [49-72] | 52 [43-60] | 64 [42-93] | 63 [52-71] | 16 [9-26] | 13 [10-17] |

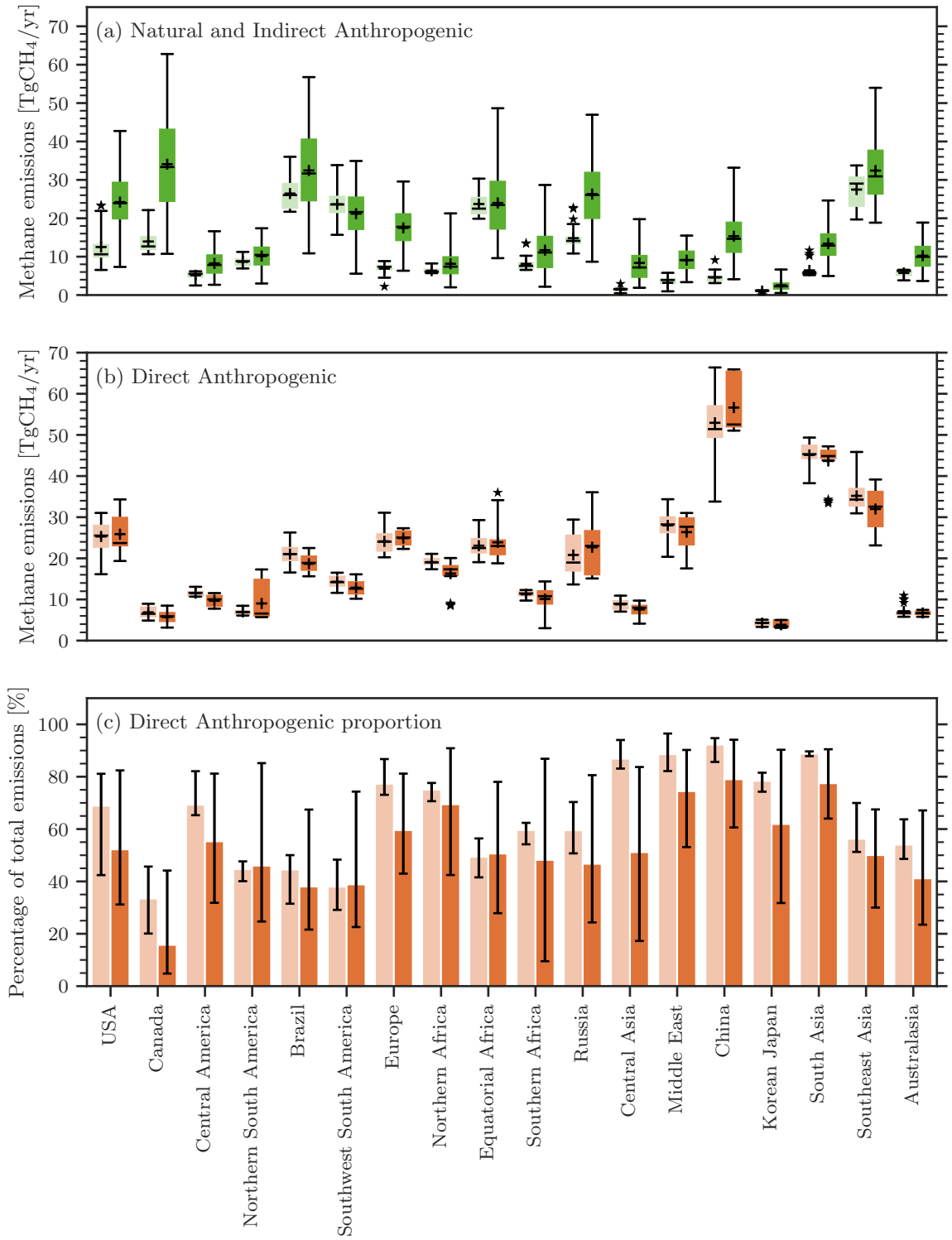


Figure S5: (a) Natural (green) emissions by region, (b) mean anthropogenic (orange), and (c) mean anthropogenic proportion as a percentage of total regional emissions (orange) in $TgCH_4\,yr^{-1}$ for 2010 – 2019 decade for top-down estimates (left light colored box plots or bars) and bottom-up estimates (right dark colored box plots or bars). Suspected outliers are marked with stars in (a) and (b) and excluded from (c), they were determined as values below the first quartile minus 3 times the inter-quartile range, or values above the third quartile plus 3 times the inter-quartile range. Mean values are represented with "+" symbols.

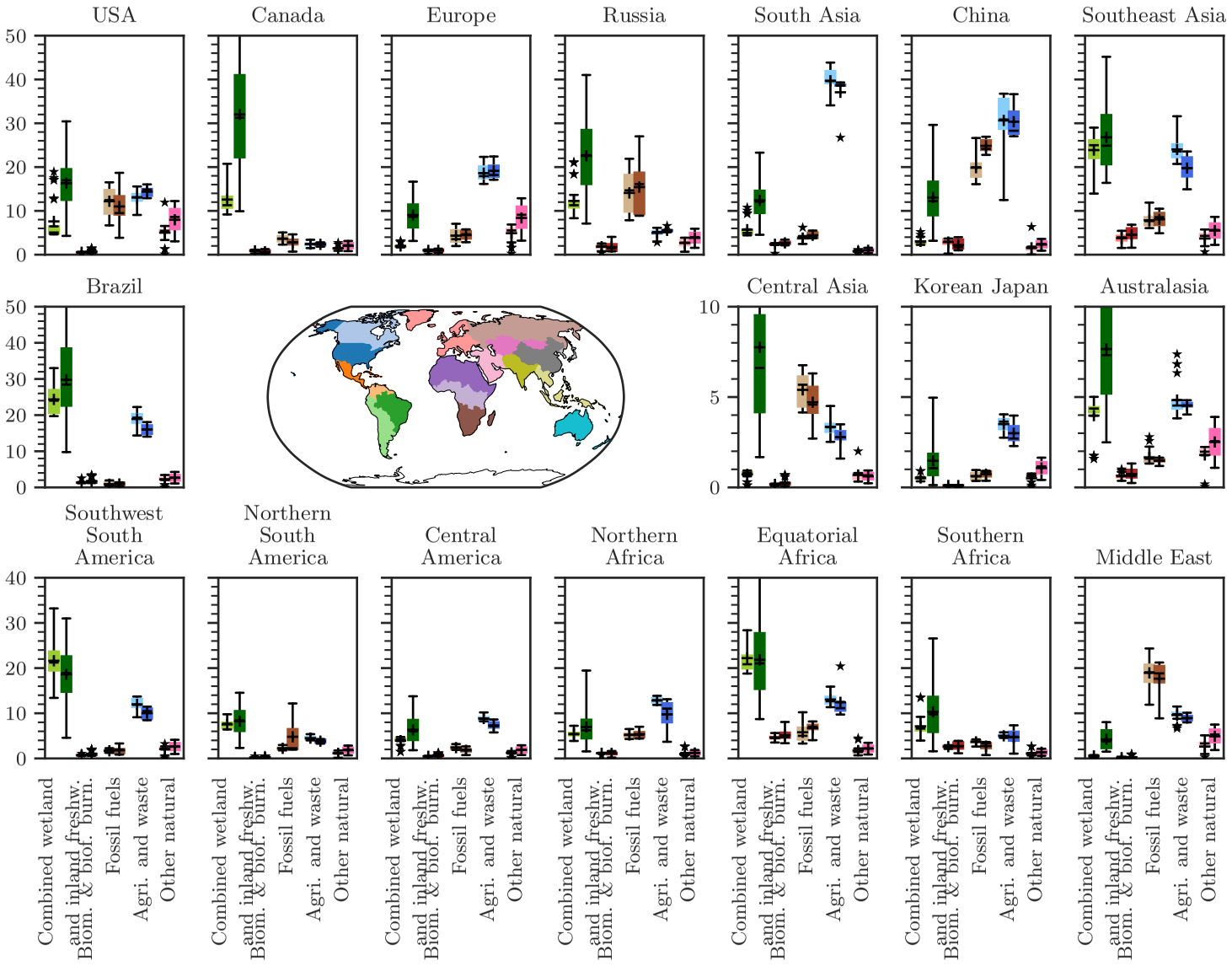


Figure S6: Regional emissions for main emissions broad categories: inland waters, fossil fuel and agriculture Waste, Biomass and Biofuel burning and Other natural emissions from top-down estimates (left boxplots and bottom-up estimates (right boxplots). The inner map shows the region's distribution. Values are given for the 2010-2019 decade.

# 9 Methane recent changes

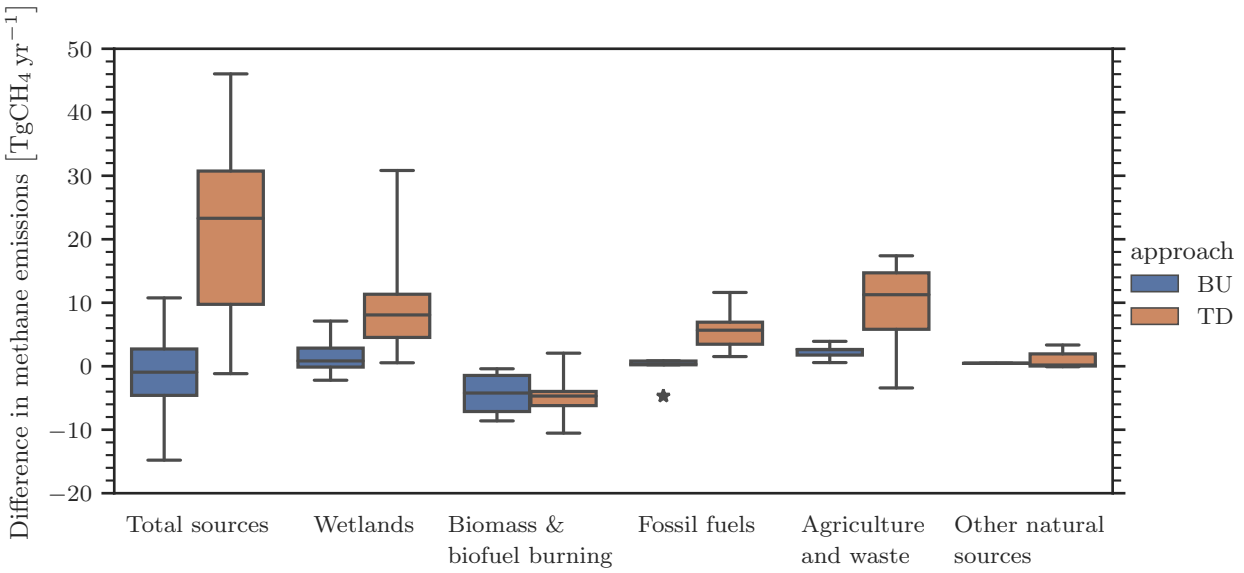


Figure S7: Difference in global emissions between 2020 and 2019 based on the ensemble of data sets contributing the bottom-up and top-down budgets.

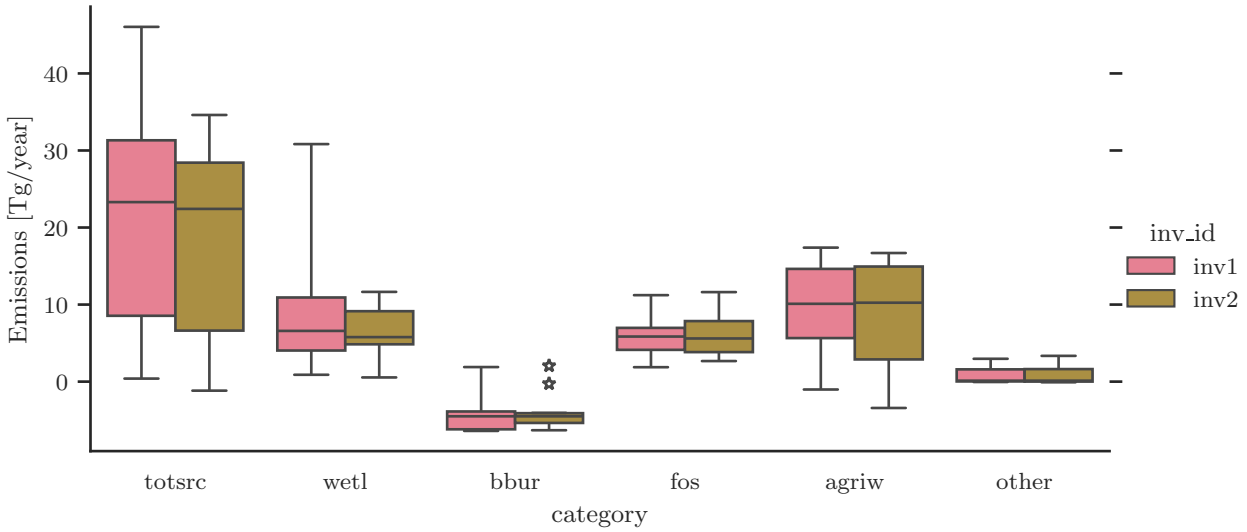


Figure S8: Difference in global emissions between 2020 and 2019 based on the top-down approaches only, for the total sources (totsrc) and wetland (wetl), biomass and biofuel burning (bbur), fossil fuels (fos), agriculture and waste (agriw), and other natural (other) emissions. Inv1 group assumed constant OH through the full period of inversion. Inv2 group assumed OH IAV based on Patra et al., (2021).

Table S19: Direct anthropogenic emissions estimated by EDGARv8 inventory for years 2020 to 2022 in $TgCH_4\,yr^{-1}$

| | 2020 | 2021 | 2022 | Difference 2022-2020 |
|---|---|---|---|---|
| Total anthropogenic emissions | 373.7 | 379.4 | 386.0 | 12.3 |
| Fossil fuel total | 118.6 | 121.6 | 126.2 | 7.6 |
| Coal | 42.2 | 43.5 | 46.8 | |
| Oil and gas | 67.7 | 68.5 | 69.8 | |
| Industry | 8.2 | 8.4 | 8.4 | |
| Transport | 1.0 | 1.0 | 1.1 | |
| Agriculture and waste total | 243.9 | 246.6 | 248.5 | 4.6 |
| Agriculture total | 159.8 | 160.9 | 161.5 | 1.7 |
| Livestock | 123.0 | 124.1 | 125.0 | |
| Rice | 36.8 | 36.9 | 36.5 | |
| Landfill and waste | 84.1 | 85.6 | 87.0 | 2.9 |
| Biofuel | 11.3 | 11.3 | 11.3 | |

# 10 TROPOMI - observations

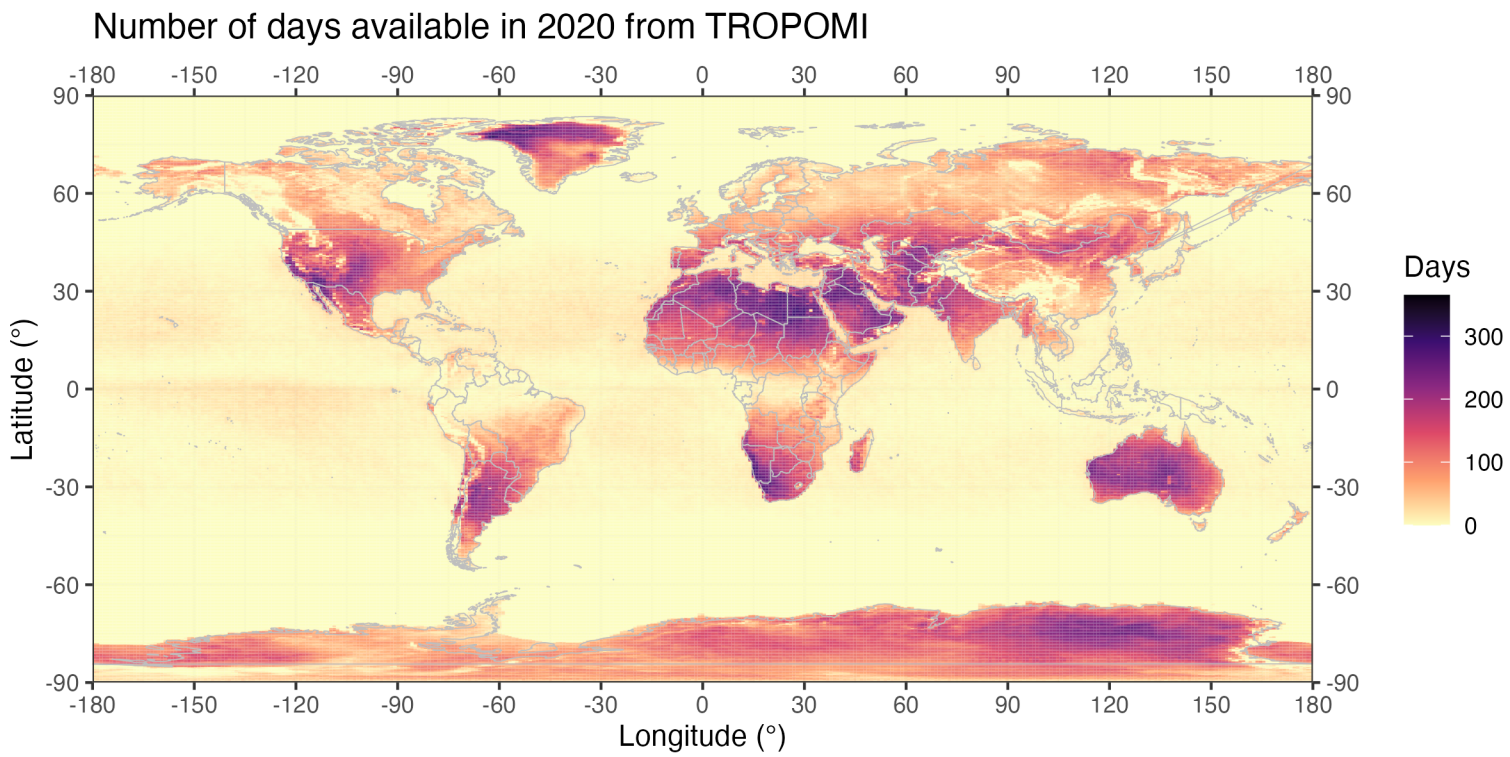


Figure S9: Number of daily observations over the year 2020 from the product Sentinel-5P TROPOMI Methane CH4 L2 5.5km x 7km, last access date Dec 1, 2023 via NASA: `https://disc.gsfc.nasa.gov/datasets/S5P_L2__CH4____HiR_2/summary?keywords=tropomi%20ch4`.

## References


Arakawa, A. and Schubert, W. H.: Interactions of cu- mulus cloud ensemble with the large-scale environment, Part I, J. Atmos. Sci., 31, 674–701, doi:10.1175/1520- 0469(1974)031¡0674:IOACCE¿2.0.CO;2, 1974.

Bergamaschi, P., Krol, M., Meirink, J. F., Dentener, F., Segers, A., van Aardenne, J., Monni, S., Vermeulen, A. T., Schmidt, M., Ramonet, M., Yver, C., Meinhardt, F., Nisbet, E. G., Fisher, R. E., O'Doherty, S., and Dlugokencky, E. J.: Inverse modeling of European CH4 emissions 2001–2006, J. Geophys. Res.-Atmos., 115, D22309, https://doi.org/10.1029/2010JD014180, 2010.

Bergamaschi, P., Houweling, S., Segers, A., Krol, M., Frankenberg, C., Scheepmaker, R. A., Dlugokencky, E., Wofsy, S. C., Kort, E. A., Sweeney, C., Schuck, T., Brenninkmeijer, C., Chen, H., Beck, V., and Gerbig, C.: Atmospheric CH4 in the first decade of the 21st century: Inverse modeling analysis using SCIAMACHY satellite retrievals and NOAA surface measurements, J. Geophys. Res.-Atmos., 118, 7350–7369, https://doi.org/10.1002/jgrd.50480, 2013.

Chen, Y. H. and Prinn, R. G.: Estimation of atmospheric methane emissions between 1996 and 2001 using a three-dimensional global chemical transport model, J. Geophys. Res.-Atmos., 111, D10307, doi:10.1029/2005JD006058, 2006.

Chevallier, F., Fisher, M., Peylin, P., Serrar, S., Bousquet, P., Breon, F. M., Chedin, A., and Ciais, P.: Inferring CO2 sources and sinks from satellite observations: Method and applica- tion to TOVS data, J. Geophys. Res.-Atmos., 110, D24309, doi:10.1029/2005jd006390, 2005.

Chevallier, F., Bréon, F. M., and Rayner, P. J.: Contribution of the Orbiting Carbon Observatory to the estimation of CO2 sources and sinks: Theoretical study in a variational data as- similation framework, J. Geophys. Res.-Atmos., 112, D09307, doi:10.1029/2006jd007375, 2007.

Chikira, M., Sugiyama, M.: A cumulus parameterization with state-dependent entrainment rate. Part I: Description and sensitivity to temperature and humidity profiles. Journal of the Atmospheric Sciences, 67(7), 2171-2193, 2010

Collins, W. J., Lamarque, J. F., Schulz, M., Boucher, O., Eyring, V, Hegglin, M. I., Maycock, A., Myhre, G., Prather, M., Shindell, D. and Smith, S.J.: AerChemMIP: quantifying the effects of chemistry and aerosols in CMIP6. Geoscientific Model Development 10, 585–607. doi:10.5194/ gmd-10-585-2017, 2017.

Crippa, M., Guizzardi, D., Solazzo, E., Muntean, M., Schaaf, E., Monforti-Ferrario, F., Banja, M., Olivier, J.G.J., Grassi, G., Rossi, S., Vignati, E.,GHG emissions of all world countries - 2021 Report, EUR 30831 EN, Publications Office of the European Union, Luxembourg, 2021, ISBN 978-92-76-41547-3, doi:10.2760/173513, JRC126363, 2021

Curry, C. L.: Modeling the soil consumption of atmospheric methane at the global scale, Glob. Biogeochem. Cycles, 21(4), GB4012, doi:10.1029/2006gb002818, 2007.

Dutaur, L. and Verchot, L. V.: A global inventory of the soil CH4 sink, Global Biogeochem. Cy., 21, GB4012, doi:10.1029/2006GB002734, 2007.

Etiope, G., Ciotoli, G., Schwietzke, S. and Schoell, M.: Gridded maps of geological methane emissions and their isotopic signature, Earth Syst Sci Data, 11(1), 1–22, doi:10.5194/essd-11-1-2019, 2019.

Fujii Y, Kamachi M: A nonlinear preconditioned quasi-newton method without inversion of a first-guess covariance matrix in variational analyses. Tellus A 55(5):450–454. https://doi.org/10.1034/j.1600-0870.2003.00030, 2003

Fujii Y: Preconditioned optimizing utility for large-dimensional analyses (POpULar). J Oceanogr 61(1):167–181. https://doi.org/10.1007/s10872-005-0029-z, 2005

Gregory, D., Morcrette, J.-J., Jakob, C., Beljaars, A. C. M., and Stockdale, T.: Revision of convection, radiation and cloud schemes in the ECMWF integrated forecasting system, Q. J. Roy. Meteorol. Soc., 126, 1685–1710, doi:10.1002/qj.49712656607, 2000.

Harada Y, Kamahori H, Kobayashi C, Endo H, Kobayashi S, Ota Y, Onoda H, Onogi K, Miyaoka K, Takahashi K: The JRA-55 reanalysis: representation of atmospheric circulation and climate variability. J Meteor Soc Jpn 94(3):269–302. https://doi.org/10.2151/jmsj.2016-015, 2016

Hmiel, B., Petrenko, V. V., Dyonisius, M. N., Buizert, C., Smith, A. M., Place, P. F., Harth, C., Beaudette, R., Hua, Q., Yang, B., Vimont, I., Michel, S. E., Severinghaus, J. P., Etheridge, D., Bromley, T., Schmitt, J., Faïn, X., Weiss, R. F. and Dlugokencky, E.: Preindustrial 14 CH 4 indicates greater anthropogenic fossil CH 4 emissions, Nature, 578(7795), 409–412, doi:10.1038/s41586-020-1991-8, 2020.

Holtslag, A. A. M., Boville, B. A.: Local versus nonlocal boundary-layer diffusion in a global climate model. Journal of climate, 6(10), 1825-1842, 1993

Ito, A. and Inatomi, M.: Use of a process-based model for assessing the methane budgets of global terrestrial ecosystems and evaluation of uncertainty, Biogeosciences, 9(2), 759–773, doi:10.5194/bg-9-759-2012, 2012.

Kaiser, S., Göckede, M., Castro-Morales, K., Knoblauch, C., Ekici, A., Kleinen, T., Zubrzycki, S., Sachs, T., Wille, C., and Beer, C.: Process-based modelling of the methane balance in periglacial landscapes (JSBACH-methane), Geosci. Model Dev., 10, 333–358, https://doi.org/10.5194/gmd-10-333-2017, 2017.

Kaminski, T., Rayner, P. J., Heimann, M., and Enting, I. G.: On ag- gregation errors in atmospheric transport inversions, J. Geophys. Res.-Atmos., 106, 4703–4715, 2001.

Kirschke, S., Bousquet, P., Ciais, P., Saunois, M., Canadell, J. G., Dlugokencky, E. J., Bergamaschi, P., Bergmann, D., Blake, D. R., Bruhwiler, L., Cameron-Smith, P., Castaldi, S., Chevallier, F., Feng, L., Fraser, A., Heimann, M., Hodson, E. L., Houwel- ing, S., Josse, B., Fraser, P. J., Krummel, P. B., Lamarque, J. F., Langenfelds, R. L., Le Quere, C., Naik, V., O'Doherty, S., Palmer, P. I., Pison, I., Plummer, D., Poulter, B., Prinn, R. G., Rigby, M., Ringeval, B., Santini, M., Schmidt, M., Shindell, D. T., Simpson, I. J., Spahni, R., Steele, L. P., Strode, S. A., Sudo, K., Szopa, S., van der Werf, G. R., Voulgarakis, A., van Weele, M., Weiss, R. F., Williams, J. E., and Zeng, G.: Three decades of global methane sources and sinks, Nat. Geosci., 6, 813–823, doi:10.1038/ngeo1955, 2013.

Kobayashi S, Ota Y, Harada Y, Ebita A, Moriya M, Onoda H, Onogi K, Kamahori H, Kobayashi C, Endo H, Miyaoka K, Takahashi K : The JRA-55 reanalysis: general specifications and basic characteristics. J Meteorol Soc Japan Ser II 93(1):5–48. https://doi.org/10.2151/jmsj.2015-001, 2015

Krol, M., de Bruine, M., Killaars, L., Ouwersloot, H., Pozzer, A., Yin, Y., Chevallier, F., Bousquet, P., Patra, P., Belikov, D., Maksyutov, S., Dhomse, S., Feng, W., and Chipperfield, M. P.: Age of air as a diagnostic for transport timescales in global models, Geosci. Model Dev., 11, 3109–3130, https://doi.org/10.5194/gmd-11-3109-2018, 2018.

Maksyutov, S., Oda, T., Saito, M., Janardanan, R., Belikov, D., Kaiser, J. W., Zhuravlev, R., Ganshin, A., Valsala, V. K., Andrews, A., Chmura, L., Dlugokencky, E., Haszpra, L., Langenfelds, R. L., Machida, T., Nakazawa, T., Ramonet, M., Sweeney, C. and Worthy, D.: Technical note: A high-resolution inverse modelling technique for estimating surface CO2 fluxes based on the NIES-TM ndash; FLEXPART coupled transport model and its adjoint, Atmospheric Chem. Phys. Discuss., 1–33, doi:10.5194/acp-2020-251, 2020.

Meirink, J. F., Bergamaschi, P., and Krol, M. C.: Four- dimensional variational data assimilation for inverse modelling of atmospheric methane emissions: method and comparison with synthesis inversion, Atmos. Chem. Phys., 8, 6341–6353, doi:10.5194/acp-8-6341-2008, 2008b.

Mellor, G. L. and Yamada, T.: A hierarchy of turbulence closure models for planetary boundary layers, J. Atmos. Sci., 31, 1791– 1806, doi:10.1175/1520-0469 031¡1791:AHOTCM¿2.0.CO;2, 1974.

Mellor, G. L. and Yamada, T.: Development of a turbulence closure model for geostrophic fluid problems, Rev. Geophys., 20, 851– 875, doi:10.1029/RG020i004p00851, 1982.

Murguia-Flores, F., Arndt, S., Ganesan, A. L., Murray-Tortarolo, G. and Hornibrook, E. R. C.: Soil Methanotrophy Model (MeMo v1.0): a process-based model to quantify global uptake of atmospheric methane by soil, Geosci. Model Dev., 11(6), 2009–2032, doi:10.5194/gmd-11-2009-2018, 2018.

Nakanishi, M., Niino, H.: An improved Mellor–Yamada level-3 model with condensation physics: Its design and verification. Boundary-layer meteorology, 112, 1-31, 2004

Niwa, Y., Ishijima, K., Ito, A. and Iida, Y.: Toward a long-term atmospheric CO2 inversion for elucidating natural carbon fluxes: technical notes of NISMON-CO2 v2021.1. Prog. Earth Planet Sci. 9, 42, doi:10.1186/s40645-022-00502-6, 2022

Oreggioni, G. D., F. Monforti Ferrario, M. Crippa, M. Muntean, E. Schaaf, D. Guizzardi, E. Solazzo, M. Duerr, M. Perry and E. Vignati: Climate change in a changing world: Socio-economic and technological transitions, regulatory frameworks and trends on global greenhouse gas emissions from EDGAR v.5.0, Global Environmental Change, doi:10.1016/j.gloenvcha.2021.10235, 2021

Pandey, S., Houweling, S., Krol, M., Aben, I., Chevallier, F., Dlugokencky, E. J., Gatti, L. V., Gloor, M., Miller, J. B., Detmers, R., Machida, T. and Röckmann, T.: Inverse modeling of GOSAT-retrieved ratios of total column CH4 and CO2 for 2009 and 2010, Atmospheric Chem. Phys. Discuss., 2016, 1–32, doi:10.5194/acp-2016-77, 2016.

Patra, P. K., Houweling, S., Krol, M., Bousquet, P., Belikov, D., Bergmann, D., Bian, H., Cameron-Smith, P., Chipperfield, M. P., Corbin, K., Fortems-Cheiney, A., Fraser, A., Gloor, E., Hess, P., Ito, A., Kawa, S. R., Law, R. M., Loh, Z., Maksyutov, S., Meng, L., Palmer, P. I., Prinn, R. G., Rigby, M., Saito, R. and Wilson, C.: TransCom model simulations of CH4 and related species: linking transport, surface flux and chemical loss with CH4 variability in the troposphere and lower stratosphere, Atmospheric Chem. Phys., 11(24), 12,813-12,837, doi:10.5194/acp-11-12813-2011, 2011.

Patra, P. K., Takigawa, M., Watanabe, S., Chandra, N., Ishijima, K. and Yamashita, Y.: Improved Chemical Tracer Simulation by MIROC4.0-based Atmospheric Chemistry-Transport Model (MIROC4-ACTM), SOLA, 14(0), 91–96, doi:10.2151/sola.2018-016, 2018.

Plummer, D., Nagashima, T., Tilmes, S., Archibald, A., Chiodo, G., Fadnavis, S., Garny, H., Josse, B., Kim, J., Lamarque, J.-F., Morgenstern, O., Murray, L., Orbe, C., Tai, A., Chipperfield, M., Funke, B., Juckes, M., Kinnison, D., Kunze, M., Luo, B., Matthes, K., Newman, P. A., Pascoe, C. and Peter, T.: CCMI- 2022: a new set of Chemistry–Climate Model Initiative (CCMI) community simulations to update the assessment of models and support upcoming ozone assessment activities. SPARC Newsletter 57, 22–30, 2021.

Poulter, B., Bousquet, P., Canadell, J. G., Ciais, P., Peregon, A., Saunois, M., Arora, V. K., Beerling, D. J., Brovkin, V., Jones, C. D., Joos, F., Gedney, N., Ito, A., Kleinen, T., Koven, C. D., McDonald, K., Melton, J. R., Peng, C. H., Peng, S. S., Prigent, C., Schroeder, R., Riley, W. J., Saito, M., Spahni, R., Tian, H. Q., Taylor, L., Viovy, N., Wilton, D., Wiltshire, A., Xu, X. Y., Zhang, B. W., Zhang, Z., and Zhu, Q. A.: Global wetland contribution to 2000–2012 atmospheric methane growth rate dynamics, Environ. Res. Lett., 12, 094013, https://doi.org/10.1088/1748-9326/aa8391, 2017.

Ridgwell, A. J., Marshall, S. J. and Gregson, K.: Consumption of atmospheric methane by soils: A process-based model, Glob. Biogeochem. Cycles, 13(1), 59–70, doi:10.1029/1998gb900004, 1999.

Riley, W. J., Subin, Z. M., Lawrence, D. M., Swenson, S. C., Torn, M. S., Meng, L., Mahowald, N. M. and Hess, P.: Barriers to predicting changes in global terrestrial methane fluxes: analyses using CLM4Me, a methane biogeochemistry model integrated in CESM, Biogeosciences, 8(7), 1925–1953, doi:10.5194/bg-8-1925-2011, 2011.

Rodgers, C. D.: Inverse methods for atmospheric sounding: the- ory and practice, Atmospheric, Oceanic and Planetary Physics, edited by: World-Scientific, Singapore, London, 240 pp., 2000.

Saunois, M., Bousquet, P., Poulter, B., Peregon, A., Ciais, P., Canadell, J. G., Dlugokencky, E. J., Etiope, G., Bastviken, D., Houweling, S., Janssens-Maenhout, G., Tubiello, F. N., Castaldi, S., Jackson, R. B., Alexe, M., Arora, V. K., Beerling, D. J., Bergamaschi, P., Blake, D. R., Brailsford, G., Brovkin, V., Bruhwiler, L., Crevoisier, C., Crill, P., Covey, K., Curry, C., Frankenberg, C., Gedney, N., Höglund-Isaksson, L., Ishizawa, M., Ito, A., Joos, F., Kim, H.-S., Kleinen, T., Krummel, P., Lamarque, J.-F., Langenfelds, R., Locatelli, R., Machida, T., Maksyutov, S., McDonald, K. C., Marshall, J., Melton, J. R., Morino, I., Naik, V., O'Doherty, S., Parmentier, F.-J. W., Patra, P. K., Peng, C., Peng, S., Peters, G. P., Pison, I., Prigent, C., Prinn, R., Ramonet, M., Riley, W. J., Saito, M., Santini, M., Schroeder, R., Simpson, I. J., Spahni, R., Steele, P., Takizawa, A., Thornton, B. F., Tian, H., Tohjima, Y., Viovy, N., Voulgarakis, A., van Weele, M., van der Werf, G. R., Weiss, R., Wiedinmyer, C., Wilton, D. J., Wiltshire, A., Worthy, D., Wunch, D., Xu, X., Yoshida, Y., Zhang, B., Zhang, Z., and Zhu, Q.: The global methane budget 2000–2012, Earth Syst. Sci. Data, 8, 697–751, https://doi.org/10.5194/essd-8-697-2016, 2016.

Saunois, M., Stavert, A. R., Poulter, B., Bousquet, P., Canadell, J. G., Jackson, R. B., Raymond, P. A., Dlugokencky, E. J., Houweling, S., Patra, P. K., Ciais, P., Arora, V. K., Bastviken, D., Bergamaschi, P., Blake, D. R., Brailsford, G., Bruhwiler, L., Carlson, K. M., Carrol, M., Castaldi, S., Chandra, N., Crevoisier, C., Crill, P. M., Covey, K., Curry, C. L., Etiope, G., Frankenberg, C., Gedney, N., Hegglin, M. I., Höglund-Isaksson, L., Hugelius, G., Ishizawa, M., Ito, A., Janssens-Maenhout, G., Jensen, K. M., Joos, F., Kleinen, T., Krummel, P. B., Langenfelds, R. L., Laruelle, G. G., Liu, L., Machida, T., Maksyutov, S., McDonald, K. C., McNorton, J., Miller, P. A., Melton, J. R., Morino, I., Müller, J., Murguia-Flores, F., Naik, V., Niwa, Y., Noce, S., O'Doherty, S., Parker, R. J., Peng, C., Peng, S., Peters, G. P., Prigent, C., Prinn, R., Ramonet, M., Regnier, P., Riley, W. J., Rosentreter, J. A., Segers, A., Simpson, I. J., Shi, H., Smith, S. J., Steele, L. P., Thornton, B. F., Tian, H., Tohjima, Y., Tubiello, F. N., Tsuruta, A., Viovy, N., Voulgarakis, A., Weber, T. S., van Weele, M., van der Werf, G. R., Weiss, R. F., Worthy, D., Wunch, D., Yin, Y., Yoshida, Y., Zhang, W., Zhang, Z., Zhao, Y., Zheng, B., Zhu, Q., Zhu, Q., and Zhuang, Q.: The Global Methane Budget 2000–2017, Earth Syst. Sci. Data, 12, 1561–1623, https://doi.org/10.5194/essd-12-1561-2020, 2020.

Schuldt, K. N., Aalto, T., Andrews, A., Aoki, S., Arduini, J., Baier, B., Bergamaschi, P., Biermann, T., Biraud, S. C., Boenisch, H., Brailsford, G., Chen, H., Colomb, A., Conil, S., Cristofanelli, P., Cuevas, E., Daube, B., Davis, K., Mazière, M. D., Delmotte, M., Desai, A., DiGangi, J. P., Dlugokencky, E., Elkins, J. W., Emmenegger, L., Fischer, M. L., Gatti, L. V., Gehrlein, T., Gerbig, C., Gloor, E., Goto, D., Haszpra, L., Hatakka, J., Heimann, M., Heliasz, M., Hermanssen, O., Hintsa, E., Holst, J., Ivakhov, V., Jaffe, D., Joubert, W., Kang, H.-Y., Karion, A., Kazan, V., Keronen, P., Ko, M.-Y., Kominkova, K., Kort, E., Kozlova, E., Krummel, P., Kubistin, D., Labuschagne, C., Langenfelds, R., Laurent, O., Laurila, T., Lauvaux, T., Lee, J., Lee, H., Lee, C.-H., Lehner, I., Leppert, R., Leuenberger, M., Lindauer, M., Loh, Z., Lopez, M., Machida, T., Mammarella, I., Manca, G., Marek, M. V., Martin, M. Y., Matsueda, H., McKain, K., Miles, N., Miller, C. E., Miller, J.B.,Moore,F., Morimoto,S.,Munro,D.,Myhre, C.L.,Mölder,M.,Müller-Williams, J.,Nichol,S.,Niwa,Y.,OD oherty,S., Obersteiner, F., Piacentino, S., Pichon, J. M., Pittman, J., Plass-Duelmer, C., Ramonet, M., Richardson, S., Rivas, P. P., Saito, K., Santoni, G., Sasakawa, M., Scheeren, B., Schuck, T., Schumacher, M., Seifert, T., Sha, M. K., Shepson, P., Sloop, C. D., Smith, P., Steinbacher, M., Stephens, B., Sweeney, C., Timas, H., Torn, M., Trisolino, P., Turnbull, J., Tørseth, K., Viner, B., Vitkova, G., Watson, A., Wofsy, S., Worsey, J., Worthy, D., Zahn, A., and di Sarra, A. G.: Multi-laboratory compilation of atmospheric methane data for the period 1983-2020; obspac_ch4_1_GLOBALVIEWplus_v4.0_2021-10-14, `https://doi.org/10.25925/20211001`, 2021.

Segers, A., Steinke, T., and Houweling, S.: Description of the CH4 Inversion Production Chain, CAMS (Copernicus Atmospheric Monitoring Service) Report.. [online] Available from: `https://atmosphere.copernicus.eu/sites/default/files/2022-10/CAMS255_2021SC1_D55.5.2.1-2021CH4_202206_production_chain_CH4_v1.pdf` (Accessed 1 february), 2022.

Tarantola, A.: Inverse problem theory, Elsevier, Amsterdam, the Netherlands, 1987.

Tian, H., Lu, C., Ciais, P., Michalak, A. M., Canadell, J. G., Saikawa, E., Huntzinger, D. N., Gurney, K. R., Sitch, S., Zhang, B., Yang, J., Bousquet, P., Bruhwiler, L., Chen, G., Dlugokencky, E., Friedlingstein, P., Melillo, J., Pan,

S., Poulter, B., Prinn, R., Saunois, M., Schwalm, C. R. and Wofsy, S. C.: The terrestrial biosphere as a net source of greenhouse gases to the atmosphere, Nature, 531(7593), 225–228, doi:10.1038/nature16946, 2016.

Thanwerdas, J., Saunois, M., Pison, I., Hauglustaine, D., Berchet, A., Baier, B., Sweeney, C., and Bousquet, P.: How do Cl concentrations matter for the simulation of CH4 and 13C(CH4) and estimation of the CH4 budget through atmospheric inversions?, Atmos. Chem. Phys., 22, 15489–15508, https://doi.org/10.5194/acp-22-15489-2022, 2022.

Tsuruta, A., Aalto, T., Backman, L., Hakkarainen, J., Laan-Luijkx, I. T. van der, Krol, M. C., Spahni, R., Houweling, S., Laine, M., Dlugokencky, E., Gomez-Pelaez, A. J., Schoot, M. van der, Langenfelds, R., Ellul, R., Arduini, J., Apadula, F., Gerbig, C., Feist, D. G., Kivi, R., Yoshida, Y. and Peters, W.: Global methane emission estimates for 2000–2012 from CarbonTracker Europe-CH4 v1.0, Geosci. Model Dev., 10(3), 1261–1289, doi:10.5194/gmd-10-1261-2017, 2017.

Vogelezang, D. H. P. and Holtslag, A. A. M.: Evaluation and model impacts of alternative boundary-layer height formulations, Bound.-Lay. Meteorol., 81, 245–269, 1996.

Wang, F., Maksyutov, S., Tsuruta, A., Janardanan, R., Ito, A., Sasakawa, M., Machida, T., Morino, I., Yoshida, Y., Kaiser, J. W., Janssens-Maenhout, G., Dlugokencky, E. J., Mammarella, I., Lavric, J. V. and Matsunaga, T.: Methane Emission Estimates by the Global High-Resolution Inverse Model Using National Inventories, Remote Sens., 11(21), 2489, doi:10.3390/rs11212489, 2019a.

Watanabe S, Hajima T, Sudo K, Nagashima T, Takemura T, Okajima H, Nozawa T, Kawase H, Abe M, Yokohata T, Ise T, Sato H, Kato E, Takata K, Emori S, Kawamiya M: MIROC-ESM 2010: model description and basic results of CMIP5-20c3m experiments. Geosci Model Dev 4(4):845–872. https://doi.org/10.5194/gmd-4-845-2011, 2011

Weber, T., Wiseman, N. A., and Kock, A.: Global ocean methane emissions dominated by shallow coastal waters, Nat. Commun., 10, 1–10, https://doi.org/10.1038/s41467-019-12541-7, 2019.

Yoshida, Y., Kikuchi, N., Morino, I., Uchino, O., Oshchepkov, S., Bril, A., Saeki, T., Schutgens, N., Toon, G. C., Wunch, D., Roehl, C. M., Wennberg, P. O., Griffith, D. W. T., Deutscher, N. M., Warneke, T., Notholt, J., Robinson, J., Sherlock, V., Connor, B., Rettinger, M., Sussmann, R., Ahonen, P., Heikkinen, P., Kyrö, E., Mendonca, J., Strong, K., Hase, F., Dohe, S., and Yokota, T.: Improvement of the retrieval algorithm for GOSAT SWIR XCO2 and XCH4 and their validation using TCCON data, Atmos. Meas. Tech., 6, 1533–1547, https://doi.org/10.5194/amt-6-1533-2013, 2013.

Zheng, B., Chevallier, F., Ciais, P., Yin, Y. and Wang, Y.: On the Role of the Flaming to Smoldering Transition in the Seasonal Cycle of African Fire Emissions, Geophys. Res. Lett., 45(21), 11,998-12,007, doi:10.1029/2018GL079092, 2018a.

Zheng, B., Chevallier, F., Ciais, P., Yin, Y., Deeter, M. N., Worden, H. M., Wang, Y., Zhang, Q. and He, K.: Rapid decline in carbon monoxide emissions and export from East Asia between years 2005 and 2016, Environ. Res. Lett., 13(4), 044007, doi:10.1088/1748-9326/aab2b3, 2018b.